Working Hypothesis, Special Laboratory Tests, Working Tools, Analysis of the Monitoring of a Pilot Embankment Built on Soft Clay in Santos with Wick Drains and its Application to the Final Design

J.P.P. Rémy, I.S.M. Martins, P.E.L. Santa Maria, V.N. Aguiar, M.E.S. Andrade

Abstract. Routine in-situ and laboratory investigations carried out for the basic design failed to provide reliable values for compressibility and consolidation parameters of soft clay layers at the site of a terminal to be built in Santos. A pilot embankment was designed and built divided in three equal areas, two with wick drains in a square mesh at spacings of 1.2 m and 2.4 m respectively and one with no drain. The basic working hypothesis adopted by the authors was that, in the field, primary and secondary consolidation occur simultaneously. High quality standard and special (long term and relaxation) oedometer tests provided reliable values of C_c, C_r and σ'_p and the OCR value of 2.1 as equivalent to the end of secondary consolidation allowing to estimate the total primary and secondary compressions of one of the most compressible layers (layer 6). No of the shelf tool is available to backanalyze the measured compression of a soft clay layer based on the adopted hypothesis. The first tool tested, the ε *vs.* $\log(\sigma'_v)$ Bjerrum type abacus with lines of equal $\dot{\varepsilon}$ values built from the oedometer tests results, proved to be non applicable. The second tool tested, the same type of abacus extrapolated from the first one for the field conditions through Taylor and Merchant's theory also proved to be non applicable. Both the third tool tested, the fitting of a theoretical Taylor and Merchant type curve to the measured compression curve in the area with no drain and the fourth tool tested, the fitting of a theoretical curve obtained through a method tailored by the authors designated "Primary Barron + secondary pseudo Taylor and Merchant" to the measured compression curves in the areas with wickdrains proved to provide excellent conformity of the theoretical and measured curves. The c_v and c_h field values thus obtained are of the same order of magnitude as the laboratory values and show the same trend to decrease when the effective stress increases, contradicting the current creed based on backanalysis through Asaoka's method, *i.e.* considering that secondary consolidation only starts after primary consolidations ends, that field c_v and c_h values are commonly 10 to 100 times higher than laboratory values. Based on their results the authors conclude that the excellent conformity of the theoretical and the measured curves obtained with the working hypothesis they adopted, the results of the laboratory tests they performed and the tools they used for the back-analysis, leads to the conclusion that the working hypothesis, the laboratory tests and the tools proved to be very efficient and trustworthy in leading to reliable compressibility and consolidation parameters of the soft clay, and will be equally efficient and trustworthy when used for the final design of the improvement of the foundation soft clay layer.

Keywords: soft clay, pilot embankment, secondary consolidation, wick drains, soil improvement.

1. Introduction

A multipurpose terminal is to be built at Barnabé Island on the Santos Channel opposite Santos Harbour as shown in Fig. 1. The total area to be filled is 800 000 m^2. Area 3 will be used for containers storage and part of it will be reclaimed underwater.

The field investigations carried out for the basic design included:

• 176 2½" diameter percussion borings with SPT at every meter, 148 of them down to refusal, covering the whole area, including the quay and the vessels access channel areas, leading to an average distance between borings over the whole project area a little smaller than 100 m by 100 m, 220 "undisturbed" samples extracted from 4" and 6" diameter borings and

• 375 vane-tests in 31 borings and

• 15 cone penetration tests (CPT) with 78 pore pressure dissipation tests.

J.P.P. Rémy, Mecasolo Engenharia e Consultoria Ltda., Nova Friburgo, RJ, Brazil. e-mail: jpremy@mecasolo.com.br.
I.S.M. Martins, Grupo de Reologia, Área de Mecânica dos Solos, COPPE, Universidade Federal do Rio de Janeiro, Rio de Janeiro, RJ, Brazil. e-mail: ian@coc.ufrj.br.
P.E.L. Santa Maria, Grupo de Reologia, Área de Mecânica dos Solos, COPPE, Universidade Federal do Rio de Janeiro, Rio de Janeiro, RJ, Brazil. e-mail: paulo.santa-maria@acergy-group.com.
V.N. Aguiar, Mecasolo Engenharia e Consultoria Ltda., Nova Friburgo, RJ, Brazil. e-mail: vitor@mecasolo.com.br.
M.E.S. Andrade, Mecasolo Engenharia e Consultoria Ltda., Nova Friburgo, RJ, Brazil. e-mail: mauricioengdb@bol.com.br.
Submitted on October 29, 2010; Final Acceptance on December 15, 2011; Discussion open until July 31, 2012.

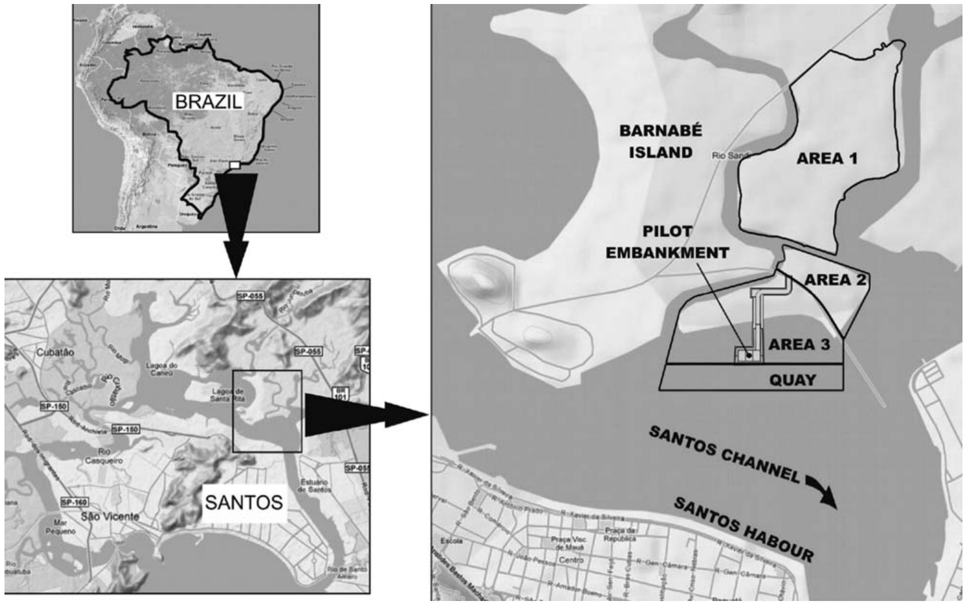

Figure 1 - Location of the container terminal.

The subsoil is rather heterogeneous and consists basically of very soft to soft clayey alluvium (SPT from 0 to 4) down to a total depth varying between 22.0 m and 43.1 m within which one or several sandy lenses or layers with SPT higher than 4 were found, mostly, with individual thicknesses of 1 to 3 m, in 83 of the 148 deep borings. The sum of these layers and lenses thicknesses is up to 2 meters in 34 borings, between 2 and 5 meters in 34 borings and between 5 and 11 meters in 15 borings.

The basic design geotechnical laboratory investigations consisted in:

• 220 grain-size distribution curves, Atterberg limits, unit weight, natural water content and specific gravity and

• 141 standard stage loading oedometer tests,

from which conservative clay layers parameters were obtained to be used for the basic design of soft soil treatment, earthworks (fills and dikes) and quay, tanks and building foundations.

2. Soil Parameters Critically Important for the Final Design and Construction of the Containers Terminal Still Not Reliably Known at the End of the Basic Design

All parameters listed in Table 1 are fairly reliable and local variations from the design values do not imply in drastic impacts on the three key points of the design which are (a) settlements values, (b) time necessary for these settlements (and the associated undrained shear strength increase) to occur and (c) fills and dikes slopes safety factors.

On the other hand, any variation of the compressibility, shear strength and consolidation parameters listed in Table 2 has a drastic impact on these key points, with special emphasis on the preconsolidation stress value which is the soil parameter with most influence on each and everyone of the three key points listed above.

A real field value of preconsolidation stress greater than the design value will lead to overestimated settlements and underestimated undrained shear strength of the soft clay. Hence, a safe design has to be based on a conservative design value of the preconsolidation stress chosen so that there be low probability of the real field value to be smaller than the design value.

On the other hand the choice of a preconsolidation stress design value on the low side may lead to a very antieconomical design due to the fact that it might require an unnecessary small spacing of wickdrains or an unnecessary thick preloading fill, or both, to meet the project deadline. This is mainly due to the fact that the value of the coefficient of consolidation in the recompression domain is usually between 30 and 100 times greater than in the virgin domain, as will be shown ahead.

The left side of Fig. 2 shows the preconsolidation stress values obtained from the 141 oedometer tests carried out for the basic design. The scattering is so high that these values could not be used to define the preconsolidation stress design profile. This is a typical example of "highly scattered lab data resulting from poor quality samples and inappropriate testing such as doubling the load in oedometer test (ill defined σ'_p)" as pointed out by Ladd (2008).

The only possible way of inferring the preconsolidation stress design profile was from the shear strength profiles given by the vane tests as shown by the two straight lines on the right side of Fig. 2. The equations of these two straight lines were used to obtain the design profile of σ'_p through the correlation between the in-situ undrained shear strength S_u, obtained from the vane test values, S_u(VT) (see

Table 1 - Physical properties of soft clay – Basic design values (*).

Depth	% < 5 μ (%)	w (%)	LL (%)	PI (%)	γ (kN/m³)	e_0
0 to 3 m						
3 to 6 m	36	73.5	78.2	47.1	15.6	2.08
6 to 9 m						
9 to 18 m	63	94.4	124.1	79.6	14.4	2.79
> 18 m	49	70.0	89.0	54.3	15.7	2.08

(*) % < 5 μ = percentage of particles smaller than 0.005 mm, w = natural water content, LL = liquid limit, PI = plasticity index, γ = unit weight, e_0 = initial void ratio (after sampling).

Table 2 - Compressibility, shear strength and consolidation parameters – Basic design values (**).

Depth	$C_c/(1 + e_0)$	C_e/C_c	σ'_p (kPa) (z in meters)	S_u (kPa) (z in meters)	S_u/σ'_p	c_h (m²/s)
0 to 3 m			1.6+4.7z	0.5+1.2z		
3 to 6 m	0.28	0.112	14+4.7z	4.0+1.2z		
6 to 9 m					0.26	2.5 x 10^{-7}
9 to 18 m	0.36	0.126	30+4.7z	9.0+1.2z		
> 18 m	0.29	0.146				

(**) C_c = compression index, C_e = expansion index, σ'_p = preconsolidation stress, S_u = undrained in-situ shear strength, c_h = horizontal coefficient of consolidation in the recompression range.

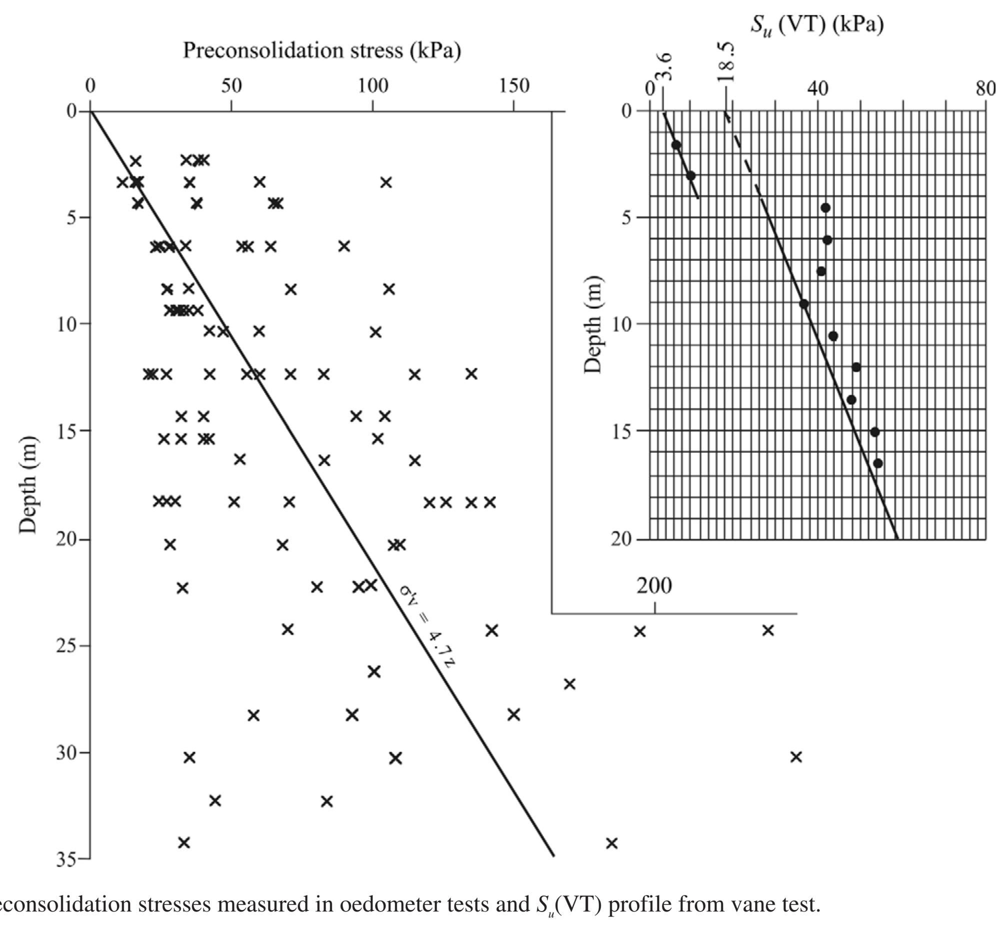

Figure 2 - Preconsolidation stresses measured in oedometer tests and S_u(VT) profile from vane test.

the right side of Fig. 2), by applying Bjerrum's reduction factor to obtain the field values S_u, and σ'_p.

3. Local Soil Profile and Soil Properties Under the Pilot Embankment

The main aim of the pilot embankment and its geotechnical investigations was to provide the best information about the consolidation characteristics of the soft clay. The embankment total length at elevation +3.00 m (which was the terminal pavement design elevation) is 150 m and its width at elevation +3.00 m is 70 m. It is divided in 3 areas as shown in Fig. 3. Area 1 is provided with a square mesh of wick drains spaced 1.20 m penetrating 30 m from elevation +1.80 m down to elevation -28.20 m. Area 2 is provided with a square mesh of wick drains spaced 2.40 m also penetrating from elevation +1.80 m down to elevation -28.20 m. Area 3 has no wick drain.

The geotechnical investigations under the pilot embankment consisted of 5 percussion borings with SPT at every meter down to refusal, three 6" borings to obtain 4" undisturbed samples for laboratory tests, 4 CPT with 28 pore pressure dissipation tests and 67 vane tests in 5 borings, as shown in Fig. 3. The water content of SPT samples was measured in the material collected close to the bottom of every sample and proved to be very helpful in defining the soil profile.

All undisturbed samples were extracted with stationary piston sampler with authors Martins and Aguiar present on the site to ensure that proper procedures were rigorously followed to provide the best possible samples quality. The 12 samples obtained in boring SRA-203 under area 3 were very carefully sealed with paraffin, wrapped, packed and transported into special manufactured wood boxes which allowed keeping them in their proper upside vertical position. These samples were transported to the soil mechanics laboratory of the Rheology Group at COPPE – UFRJ where they were tested. The test program consisted of unit weight, natural water content, specific gravity, grain size analysis, Atterberg limits and organic matter content for each sample. 42 standard and 32 special oedometer tests were performed under controlled temperature by Aguiar (2008) and Andrade (2009) on 70 mm diameter, 20 mm height specimens. The specimens were prepared according to Ladd and DeGroot (2003) recommendations. Figure 4 shows the results of 7 oedometer tests carried out on undisturbed specimens trimmed in sample number 6 and the result of one test carried out on a remoulded specimen prepared from the same sample.

In respect to Coutinho's (2007) samples quality classification criteria, all specimens from layer 6, save two specimens in sample SRA-203(10) and one in sample SRA-203(5), were classified as excellent to fair.

Figure 5 shows the soil profiles below the centers of areas 3, 2 and 1 as established based on the results of all field and laboratory soil investigations carried out in the subsoil under the pilot embankment. The figure shows the stratigraphy with each layer description, the SPT values, the positions of the undisturbed samples and the positions of the settlement measuring magnets. In area 3, it also shows the initial vertical effective stress profile (σ'_v) and the preconsolidation stress profile (σ'_p) obtained from the oedometer tests performed on SRA-203 samples as dis-

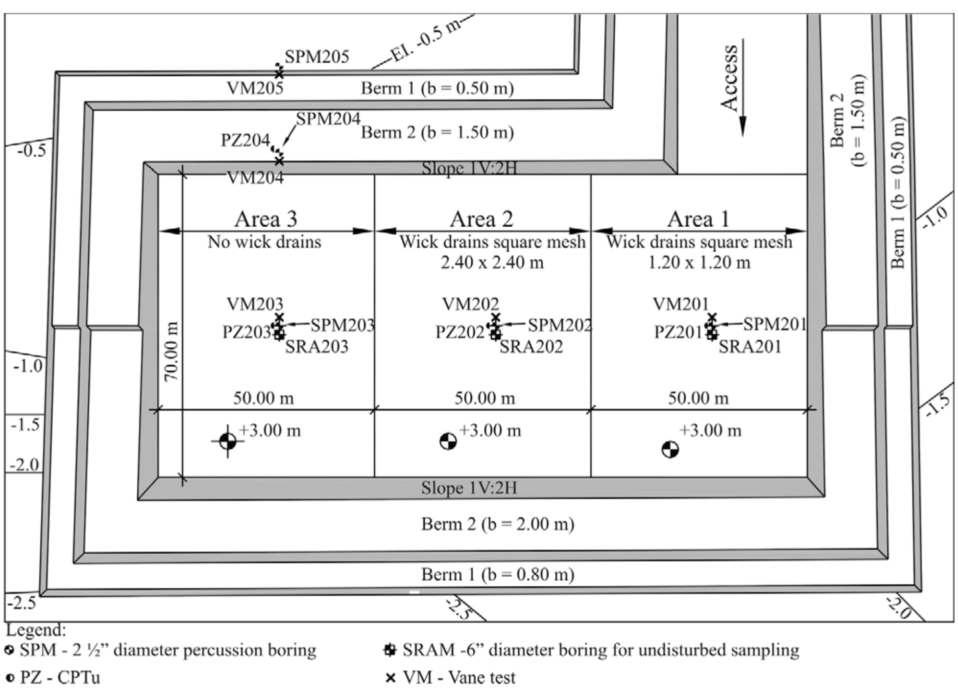

Figure 3 - Pilot embankment soil investigations location.

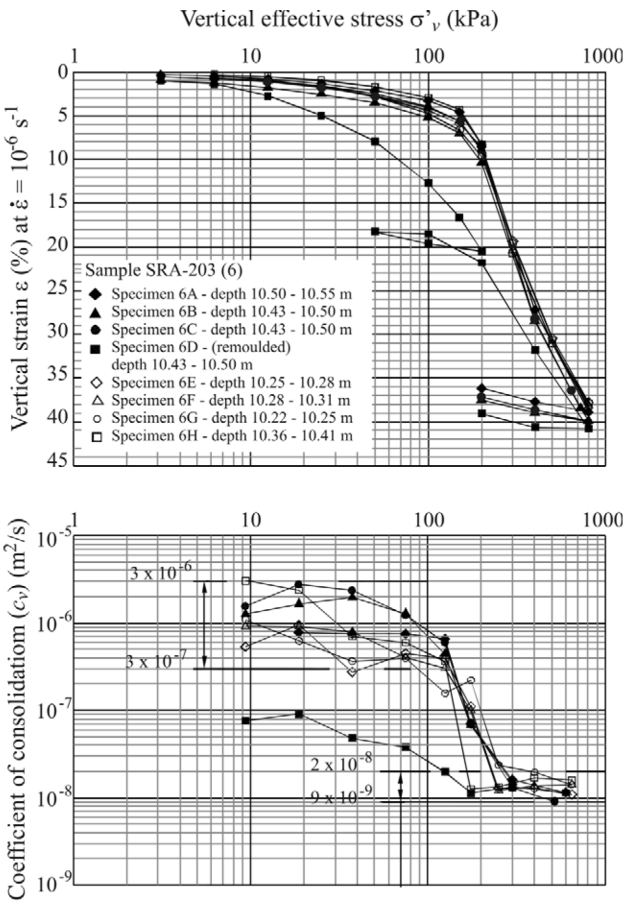

Figure 4 - Results of standard oedometer tests on sample number 6 of boring SRA-203.

cussed ahead. As shown in Fig. 6, the preconsolidation stresses obtained at strain rate $\dot{\varepsilon}_v = 10^{-6}$ s^{-1} from the good quality samples tested at COPPE were much higher than the adopted values for the basic design, the same being true for the $C_c/(1 + e_0)$ values. Andrade (2009) observed that the σ'_p values at $\dot{\varepsilon}_v = 10^{-6}$ s^{-1} are, in average, 8% higher than the σ'_p values determined for 24 h loading stages. The authors consider these COPPE values to be very reliable since the same high repeatability of the results shown in Fig. 4 was obtained on all the clayey samples of SRA-203, and very good repeatability, although not as high, was obtained on the more sandy samples. The samples taken from borings SRA-201 and SRA-202 were tested in another laboratory and their results which indicate that the specimen tested were of lower quality than the ones tested at COPPE are not included in the present analysis.

To define the σ'_p profile, a line passing through the highest σ'_p experimental values was chosen considering that these correspond to the highest quality specimens since any degree of remoulding of the samples lowers the value of σ'_p.

Table 3 shows the soils properties defined from the soils investigations carried out in the foundation of the pilot embankment, including the physical properties of samples from SRA-201 and SRA-202.

4. Pilot Embankment Construction History and Instrumentation

The pilot embankment construction was very carefully planned and carried out to avoid any local failure of the extremely soft clay layer (layer 1) which extends down to 1.5 to 2 meters depth. At first, nonwoven geotextile was laid on top of the soft clay layer, covering the whole area. Then a 15 to 30 cm thick layer of quarry dust was hydraulically carefully spread into place. This layer was covered with a geogrid with a strength of 800 kN/m and the fill material was slowly put into place, first being dumped under the water level and then as soon as access was possible at low tide, poured by trucks and bulldozers. When elevation + 1.80 m was reached, the wick drains were driven down to their design depth of 30 m below embankment level, requiring that holes be first drilled through the embankment and the geogrid. The embankment was then completed up to elevation +3.00 m as shown in Fig. 3.

Table 3 - Soils properties from the soils investigations of the pilot embankment (*).

Layer(**)	γ (kN/m^3)	$C_c/(1 + e_0)$	C_s/C_c	c_{v1} (m^2/s)	c_{v2} (m^2/s)	c_{h1} (m^2/s)
1	13.0	0.36	0.12	-	-	-
2	20.0	-	-	-	-	1.5 x 10^{-4}
3	16.5	0.28	0.19	1.7 x 10^{-6}	6.0 x 10^{-7}	1.0 x 10^{-6}
4	17.6	0.16	0.27	1.4 x 10^{-6}	1.5 x 10^{-6}	8.3 x 10^{-6}
5	16.5	0.28	0.19	1.7 x 10^{-6}	6.0 x 10^{-7}	1.0 x 10^{-6}
6	15.0	0.56	0.11	6.5 x 10^{-7}	1.5 x 10^{-8}	4.9 x 10^{-7}
7	18.1	0.16	0.27	1.5 x 10^{-6}	1.3 x 10^{-6}	2.1 x 10^{-5}
8	14.6	0.56	0.11	6.5 x 10^{-7}	1.5 x 10^{-8}	4.9 x 10^{-7}

(*) c_{v1} and c_{h1} are for $\sigma'_v \le \sigma'_p$, and c_{v2} is for $\sigma'_v > \sigma'_p$ (c_{v1} and c_{v2} from oedometer tests, c_{h1} from CPT porepressure dissipation tests).
(**) for identification of each layer see Fig. 5.

After obtaining the first COPPE oedometer tests high preconsolidation stress values, it was decided to heighten the pilot embankment in order to apply a vertical stress higher than the preconsolidation stress. Figure 7 shows the highest embankment elevations in each area and the dates when they were reached as well as the locations of the set-

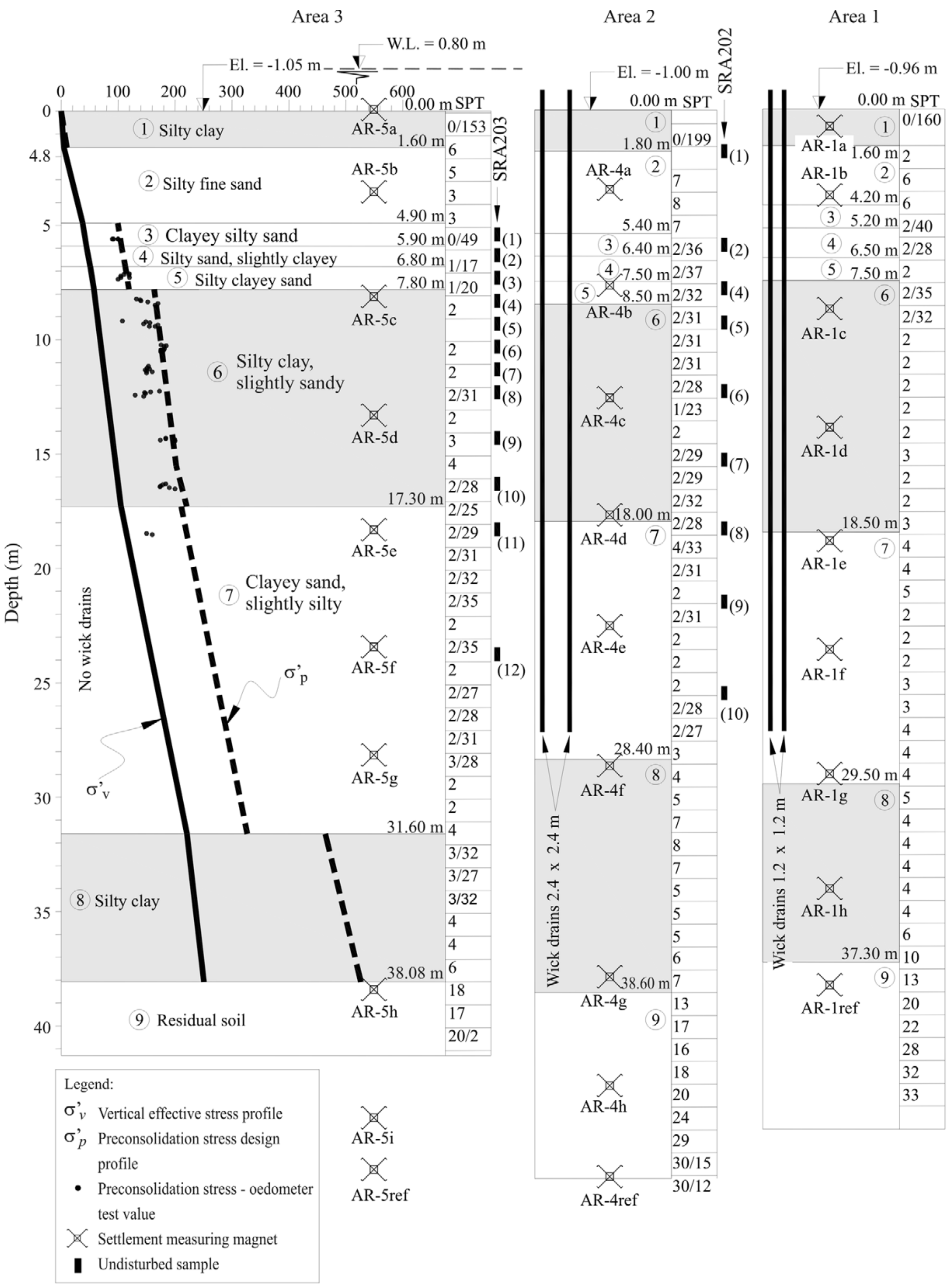

Figure 5 - Soil profiles under areas 3, 2 and 1 with positions of undisturbed samples and settlement measuring magnets.

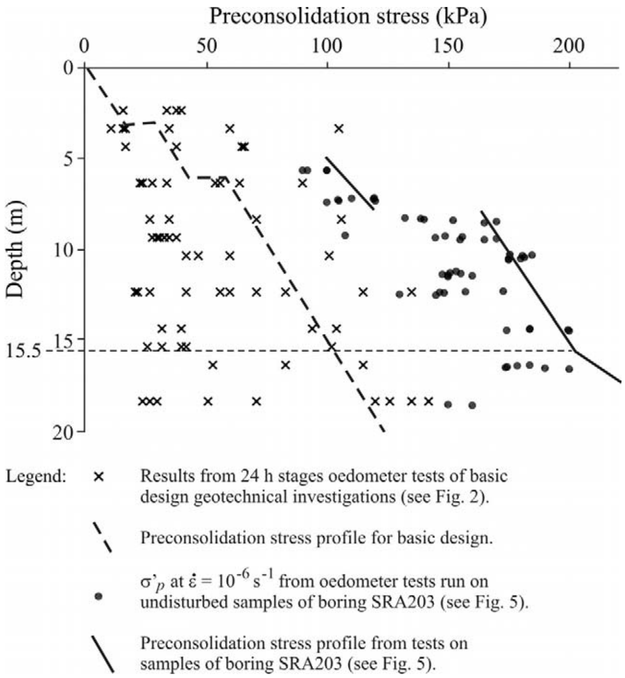

Figure 6 - Preconsolidation stress values and profiles.

tlement plates (PR), magnetic settlement gauges (MR) and inclinometers (IN) installed to monitor settlements, layers compressions and horizontal displacements, respectively.

When the decision to increase the embankment thickness was taken, the north half of area 3 had already been heightened to elevation +7.77 m, immediately after the embankment was completed to design elevation +3.00 m, with the aim to provoke a foundation failure towards inclinometers IN1, IN2 and IN3. While the heightening of the fill of the north half of area 3 was taking place, the stresses in the geogrid in the north south direction were measured with the installed strain gauges. The embankment did not show apparent deformations, almost no stress change was recorded in the strain gauges and very little lateral displacements were registered in the inclinometers. The analysis of this behaviour will not be discussed here because this subject is beyond the scope of the present work.

The pilot embankment was also instrumented with full profile hydraulic settlement gauges, electrical piezometers and open pipe piezometers, but these instruments, along with the inclinometers and the strain gauges of the geogrid were read for only a short period of time, too short to provide helpful data.

5. Special Laboratory Tests

26 long term oedometer tests were carried out. In some of them secondary consolidation was observed after unloading. Stress relaxation tests where the vertical displacements were restrained and the vertical stress measured were also carried out.

At the top of Fig. 8 are shown the results of oedometer tests run on 4 specimens trimmed in sample SRA-203(8), all consolidated under 800 kPa following the same procedure, and then unloaded to different stress values, generating different values of OCR. The specimens strains were then measured for 20 days under constant stress and constant temperature (20 °C ± 1°).

The results at the bottom of Fig. 8 show that after about 4000 min the specimen unloaded to OCR value of 1.60 stopped expanding and started to compress whereas

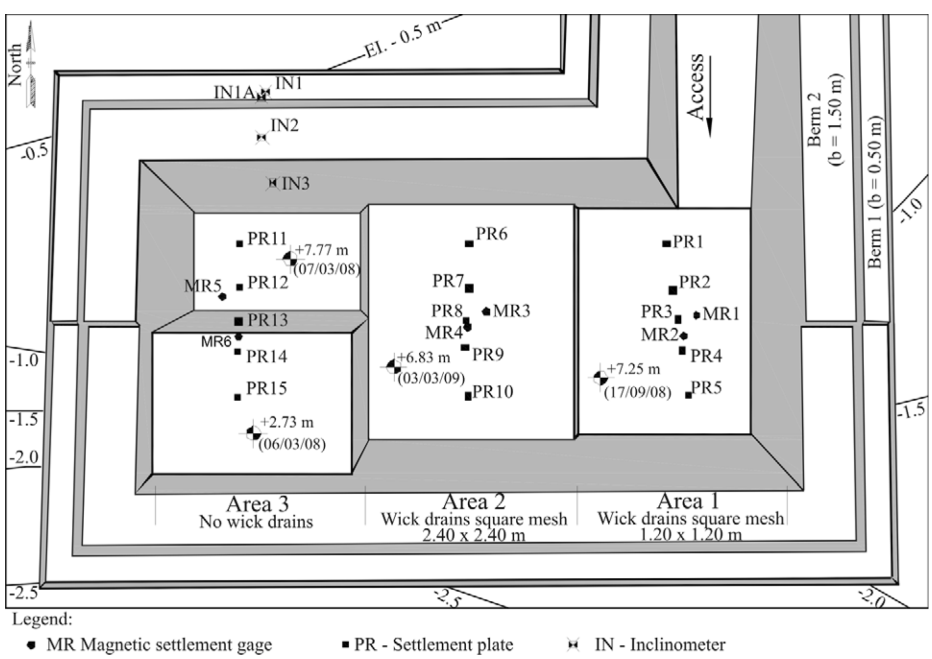

Figure 7 - Location of instruments for settlements, layer compressions and horizontal displacements measurements.

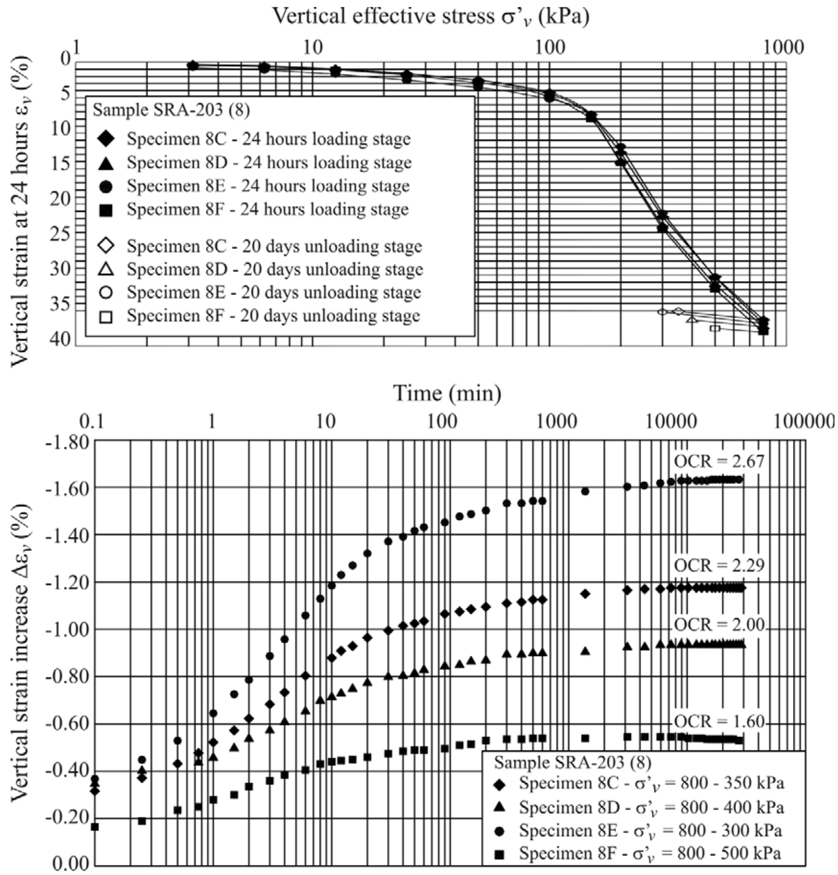

Figure 8 - Results of oedometer tests.

the specimens unloaded to OCR values of 2.00, 2.29 and 2.67 leveled off. Based on these and all other results from long term oedometer tests performed on other samples, Andrade (2009), following the procedure suggested by Feijó & Martins (1993), established that the end of secondary compression line could be drawn as being the line equivalent to an OCR value of 2.1 relative to the $\dot{\varepsilon} = 10^{-6}$ s^{-1} line. In their analysis the authors did not discriminate between the $\dot{\varepsilon} = 10^{-6}$ s^{-1} line and the end of primary compression line due to the proximity of these two lines observed in all oedometer tests results. This value can be compared to the equivalent OCR value close to 2.0 relative to E.O.P. found by Feijó (1991) for the end of secondary compression of Sarapuí clay in Rio de Janeiro, and to 1.7 relative to 24 h stages published by Martins *et al.* (2009) for various Rio de Janeiro soft clays.

The preconsolidation stresses σ'_p in layers 3, 4, 5, and 6 were established based on the oedometer tests results as seen on Fig. 6. It can be seen that, in layer 6, above 15.5 m depth the lab results show σ'_p values higher than 2.1 σ'_v leading to the conclusion that the preconsolidation is due to dune effect (Massad 1989). The same dune effect was considered to prevail in clayey sand layer 7 and the secondary compression preconsolidation effect was considered to be the predominant one in layer 1 and in layer 8 adopting $\sigma'_p = 2.1\ \sigma'_v$.

6. Pilot Embankment Monitoring Data

Due to the lack of readings of the other instruments, the monitoring data analyzed to assess the behaviour of the soft marine clay under the pilot embankment is limited to the settlement data provided by the settlement plates and the magnetic settlement gauges. Figure 9 shows the evolution of the elevation of the top of the embankment with time and the evolution of the total settlements in the center of area 1 measured through settlement plate PR3, in the center of area 2 measured through settlement plate PR8 and close to the center in area 3 measured through settlement magnet AR-5a of gauge MR5 for lack of readings of damaged settlement plate PR13.

The last points of the settlement curves above correspond to the values measured in october 5th of 2009 for settlements plates PR3 and PR8 and in october 2nd of 2009 for MR5, that is about 730 days (*i.e.* 2 years) after the beginning of construction. The values of the settlements and settlement rates measured in early october 2009 are shown in Table 4.

Figure 10 shows the evolution of the elevation of the top of the embankment with time and the evolution of the compression of layers 1, 2, 3, 4 and 5 altogether in the three areas. Figure 11 shows the evolution of the elevation of the top of the embankment with time and the evolution of layer 6 compression in the three areas. Figure 12 shows the evolution of the elevation of the top of the embankment with time and the evolution of the compression of layers 7 and 8 altogether in the three areas.

Table 5 shows the values of measured layers compressions and compression rates and of calculated strains and strain rates in october 2009.

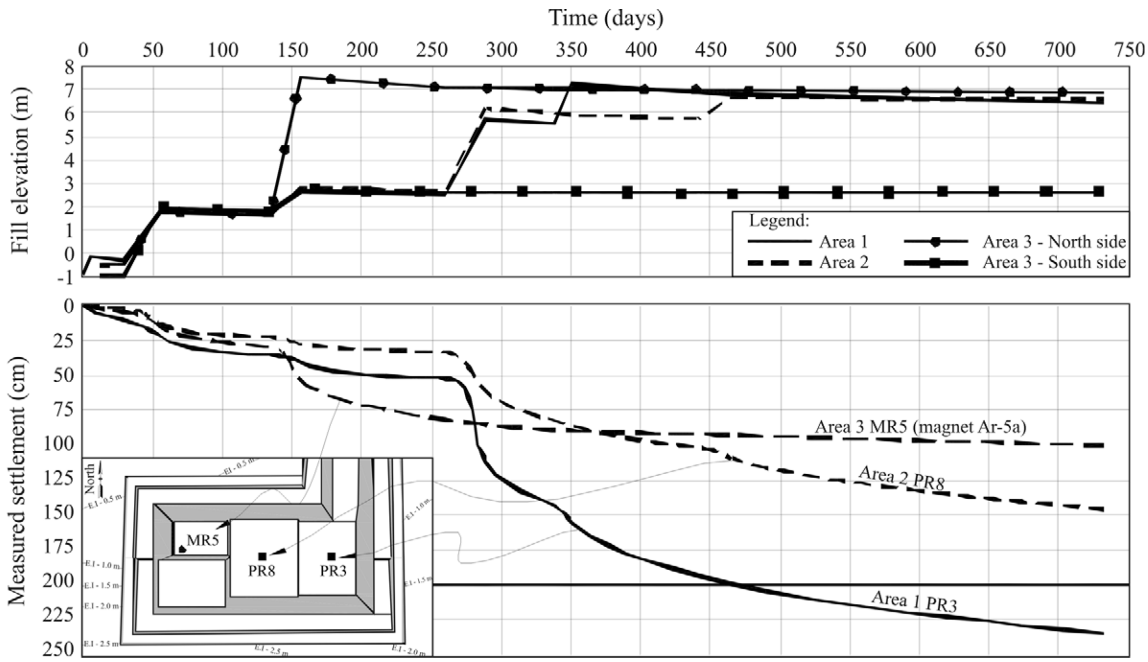

Figure 9 - Measured total settlements in the foundation.

Table 4 - Foundation settlements and settlement rates in early october 2009.

Area	Settlement	Strain	Settlement rate	Strain rate
1	236 cm	Not applicable	3.2 cm per month	Not applicable
2	146 cm	Not applicable	2.9 cm per month	Not applicable
3	101 cm	Not applicable	0.8 cm per month	Not applicable

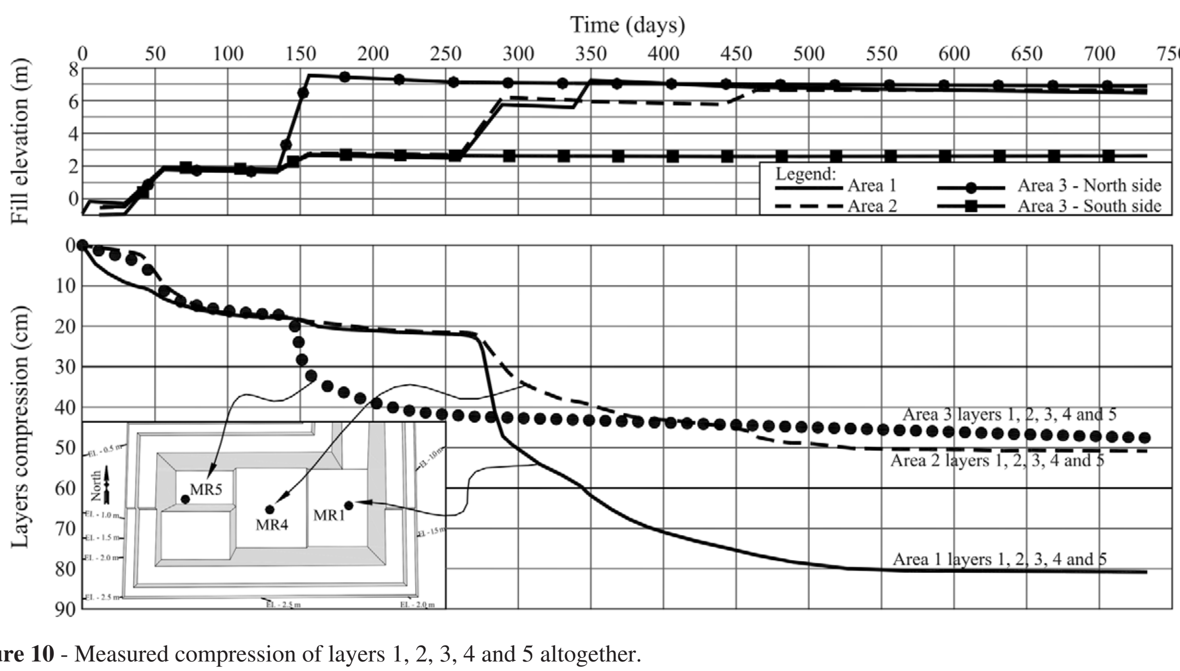

Figure 10 - Measured compression of layers 1, 2, 3, 4 and 5 altogether.

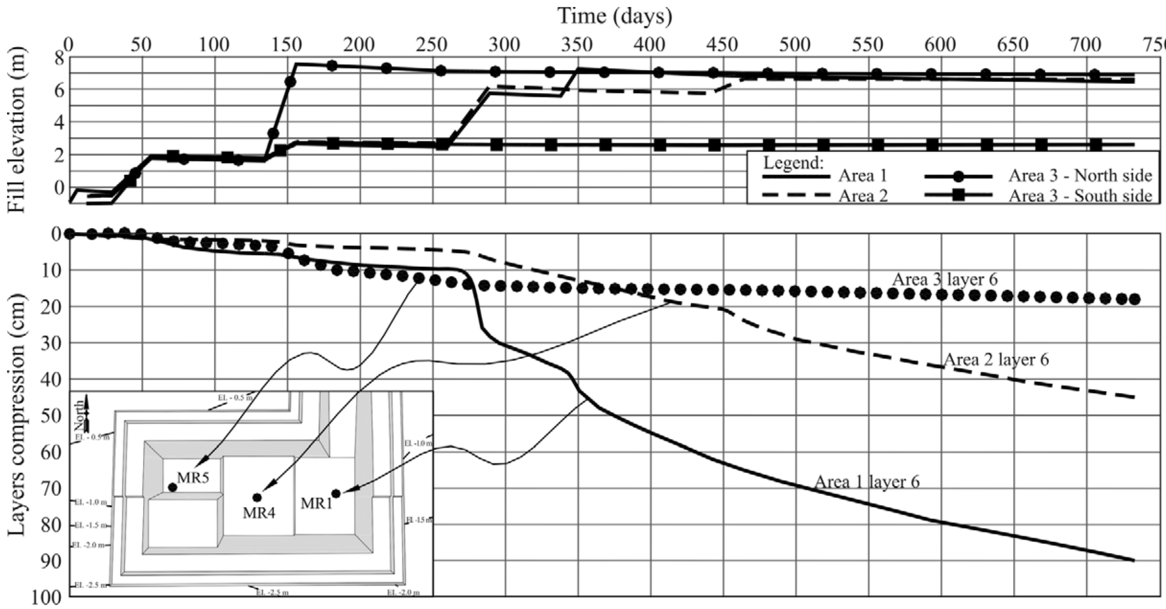

Figure 11 - Measured compression of layer 6.

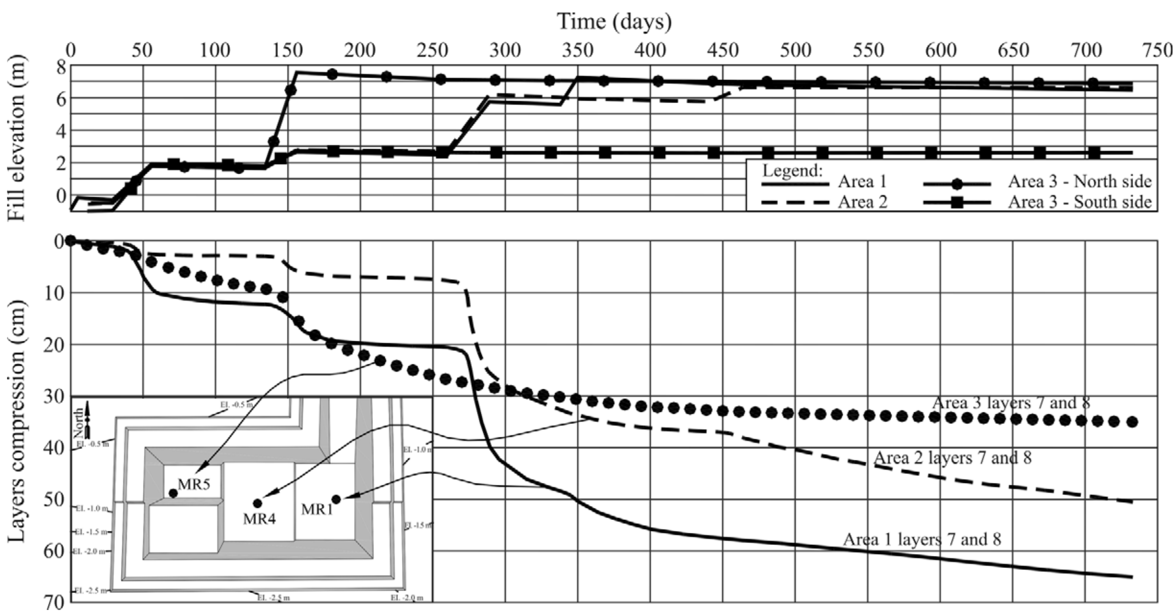

Figure 12 - Measured compression of layers 7 and 8 altogether.

7. Primary Compression and Secondary Compression

In order to analyze the settlement data presented in Figs. 9 to 12, the vertical stress increase and the final vertical effective stress (compared to the preconsolidation stress) have to be known. Figure 13 shows the profiles of final vertical stress increases calculated under the centers of areas 1, 2 and 3. The stress increase calculations were done considering the Holl (1940) formulas, apud Poulos & Davis (1974), to compute $\Delta\sigma$ at depth z under the corner of loaded rectangles. As can be seen, the stress increases are different under each area.

Figure 13 also shows the final effective vertical stresses under the centers of the three areas compared to the profiles of preconsolidation stresses. The term "final" used to characterize both vertical stresses and vertical stress increases means the values calculated for the final situation reached after full completion and stabilization of both primary and secondary consolidation settlements, taking into consideration the effect of the progressive partial submersion on the final stresses as the embankment settles. In order to obtain these "final" values, calculations had to be

Table 5 - Values of measured layers compressions and compression rates and of calculated strains and strain rates in early october 2009.

Layers	Compression (cm)			Compression rate (cm/month)		
	Area 1	Area 2	Area 3	Area 1	Area 2	Area 3
1, 2, 3, 4, 5(*)	80.8	50.9	47.6	0.1	0.1	0.3
6	90.0	45.0	18.0	2.5	1.7	0.3
7, 8(**)	65.1	50.5	35.0	0.6	1.1	0.2
Layers	Strain (%)			Strain rate (s^{-1})		
	Area 1	Area 2	Area 3	Area 1	Area 2	Area 3
1, 2, 3, 4, 5(*)	10.8	6.0	6.1	5.8×10^{-11}	4.8×10^{-11}	1.6×10^{-10}
6	8.2	4.7	1.9	9.5×10^{-10}	7.2×10^{-10}	1.2×10^{-10}
7, 8(**)	3.5	2.5	1.7	1.3×10^{-10}	2.1×10^{-10}	3.8×10^{-11}

(*) Most of the compression still in process is believed to occur predominantly in layer 1.
(**) Most of the compression still in process is believed to occur predominantly in layer 8.

done by successive iterations converging step by step to the final values.

In area 1, the final effective vertical stresses are clearly higher than the preconsolidation stresses σ'_p in layers 1, 3, 4 and 5, a little higher than σ'_p in layers 6 and 7 and much smaller than σ'_p in layer 8. In area 2, the final effective vertical stresses are clearly higher than σ'_p in layers 1, 3, 4 and 5, about equal to σ'_p in layers 6 and 7 and much smaller than σ'_p in layer 8. In the center of area 3, the final effective vertical stresses are higher than σ'_p in layers 1, 3, 4 and 5, smaller than σ'_p in layers 6 and 7 and much smaller than σ'_p in layer 8.

Figure 14 illustrates the way primary compression and secondary compression were computed. The case in which the final effective vertical stress is lower than the preconsolidation stress is shown at the top of the figure and the case in which the final effective vertical stress is higher than the preconsolidation stress is shown at the bottom.

The following terminology is used in Fig. 14: e_i = initial void ratio; σ'_{vi} = initial vertical effective stress; $\Delta\sigma_v$ = vertical stress increase; σ'_{vf} = final vertical effective stress; σ'_p = preconsolidation stress; e_p = final void ratio at the end of primary consolidation (without secondary); e_s = final ratio at the end of primary and secondary consolidation; Δe_p = variation of void ratio corresponding to primary compression and Δe_s = variation of void ratio corresponding to secondary compression.

Primary compression was computed through the common well known formulas using C_r and C_c in the recompression and virgin compression ranges respectively, and secondary compression was computed through the following formulas.

$$\Delta H_s = 0 \text{ when } \sigma'_{vf} \le \frac{\sigma'_p}{2.1} \quad (1)$$

$$\Delta H_s = H \frac{C_c}{1+e_0}\left(1-\frac{c_e}{c_c}\right)\log\left(2.1\frac{\sigma'_{vf}}{\sigma'_p}\right) \text{ when } \frac{\sigma'_p}{2.1} \le \sigma'_{vf} \le \sigma'_p \quad (2)$$

and

$$\Delta H_s = H \frac{C_c}{1+e_0}\left(1-\frac{c_e}{c_c}\right)\log(2.1) \text{ when } \sigma'_{vf} \ge \sigma'_p \quad (3)$$

For settlements evaluation purposes each layer was divided in 1 m thick sublayers.

The preconsolidation stresses and calculated final effective vertical stresses at mid-height of each whole layer, primary compressions and secondary compressions of layers 1 to 8 are shown in Tables 6, 7 and 8.

All the above compressions were computed considering all the soil mass between the drains in areas 1 and 2 to be perfectly undisturbed. It is the authors understanding that the existence of any remoulded zone around the drains would lead to higher settlements as clearly illustrated by Fig. 4. The discussion of this subject is beyond the scope of the present work.

As shown in Table 6, in area 1 the total compression of layer 6 equal to 2.20 m amounts to 52% of the total settlement equal to 4.20 m. As shown in Table 7, in area 2 the total compression of layer 6 equal to 1.78 m amounts to 46% of the total settlement equal to 3.89 m and as shown in Table 8, in area 3 the total compression of layer 6 equal to 1.38 m amounts to 48% of the total settlement equal to 2.89 m. Layer 1 comes second to layer 6 in the ranking of the layers which most contribute to the total settlement with 20%, 24% and 27% of the total settlement in areas 1, 2 and 3, respectively. In layer 1, no "undisturbed sample" could be retrieved in the very soft mud which constitutes this layer, as can be seen in Fig. 5, which means that no data about compressibility and consolidation properties could be obtained in the laboratory concerning layer 1. On the other hand, 7 "undisturbed samples" were retrieved in

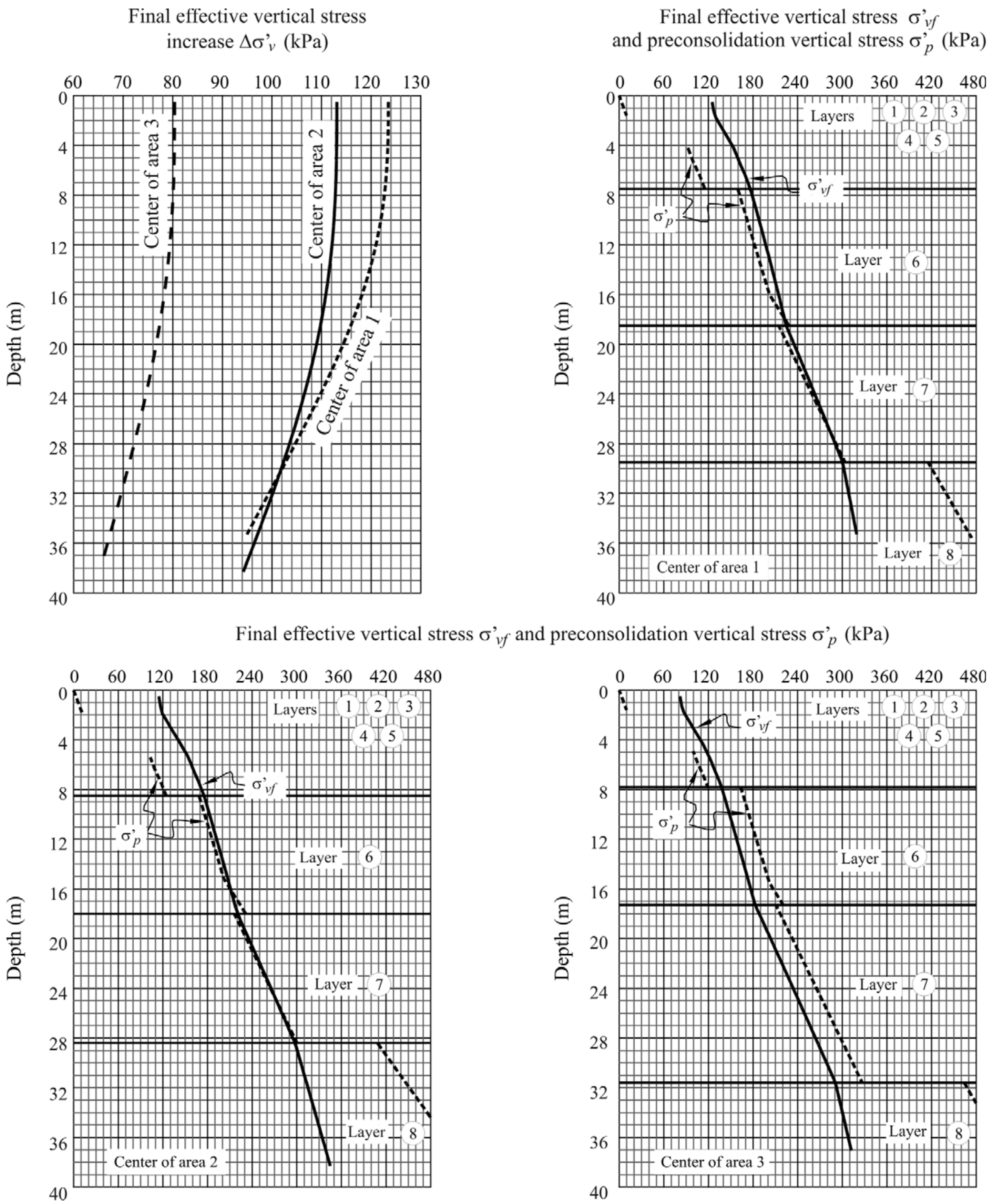

Figure 13 - Vertical stress increases and final effective vertical stresses under the centers of areas 1, 2 and 3.

layer 6 under area 3 and tested at COPPE which provided very good data for this layer. For these two reasons, the back-analysis presented in this paper is relative only to layer 6.

8. Drainage Conditions of Subsoil Layers

From the knowledge of the soil profiles and of the soil properties, the authors consider that the drainage conditions of the subsoil layers in areas 1, 2 and 3 are the ones described in Table 9.

9. Working Hypothesis

For the last 30 years or so, the main trend of thought of the most prolific brazilian researchers in the study of the behaviour of marine Santos soft clay has sustained that secondary consolidation only starts to take place at the end of

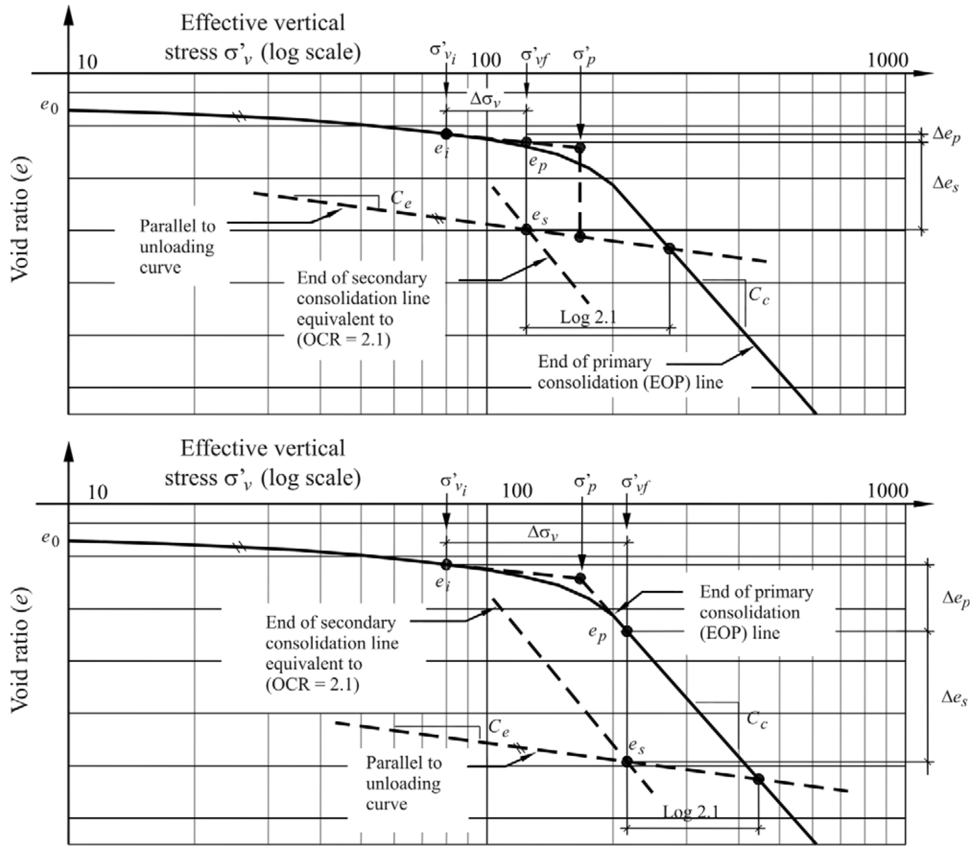

Figure 14 - Primary compression and secondary compression.

Table 6 - Preconsolidation stresses and calculated final effective vertical stresses at mid height of each layer and primary compressions and secondary compressions in area 1.

	Layer 1	Layer 2	Layer 3	Layer 4	Layer 5	Layer 6	Layer 7	Layer 8	Total
σ'_{vf}	125.9	141.3	157.4	165.4	173.4	201.6	263.1	310.5	
σ'_{p}	5.0		95.7	103.8	112.1	187.1	259.2	446.7	
ΔH_p	0.67			0.22 (*)		0.43	0.23	0.06	1.61
ΔH_s	0.16			0.15 (*)		1.77	0.00	0.51	2.59
ΔH_t	0.83			0.37 (*)		2.20	0.23	0.57	4.20
$\Delta H_m/\Delta H_t$	65%			71% (*)		41%	82% (**)	82% (**)	56%

Table 7 - Preconsolidation stresses and calculated final effective vertical stresses at mid height of each layer and primary compressions and secondary compressions in area 2.

	Layer 1	Layer 2	Layer 3	Layer 4	Layer 5	Layer 6	Layer 7	Layer 8	Total
σ'_{vf}	115.8	136.5	157.6	165.0	172.3	198.3	259.5	322.4	
σ'_{p}	5.7		106.3	113.4	121.2	192.5	258.4	470.8	
ΔH_p	0.76			0.17 (*)		0.26	0.21	0.06	1.46
ΔH_s	0.18			0.15 (*)		1.53	0.00	0.58	2.43
ΔH_t	0.94			0.32 (*)		1.79	0.21	0.64	3.89
$\Delta H_m/\Delta H_t$	31%			66% (*)		25%	60% (**)	60% (**)	38%

Table 8 - Preconsolidation stresses and calculated final effective vertical stresses at mid height of each layer and primary compressions and secondary compressions in area 3.

	Layer 1	Layer 2	Layer 3	Layer 4	Layer 5	Layer 6	Layer 7	Layer 8	Total
σ'_{vf}	82.8	101.7	121.3	127.9	134.5	160.6	237.4	301.6	
σ'_p	5.0		102.7	109.3	116.0	187.3	268.8	492.2	
ΔH_p	0.61			0.10 (*)		0.18	0.15	0.04	1.08
ΔH_s	0.16			0.15 (*)		1.20	0.00	0.30	1.81
ΔH_t	0.77			0.25 (*)		1.38	0.15	0.34	2.89
$\Delta H_m/\Delta H_t$	36%			77% (*)		13%	72% (**)	72% (**)	35%

(*) layers 3, 4 and 5 altogether.
(**) layers 7 and 8 altogether.
where: σ'_{vf} = final vertical effective stress at mid-height of whole layer (kPa), σ'_p = preconsolidation stress at mid-height of whole layer (kPa), ΔH_p = layer primary compression (m), ΔH_s = layer secondary compression (m), ΔH_t = layer total compression (m), ΔH_m = measured layer compression (m) in october 2009.

Table 9 - Drainage conditions of subsoil layers.

Layer(s)	Soil type	SPT	Areas 1 and 2 (Drains down to El. – 28.20 m)	Area 3 (No drain)
1	Silty clay	0	Double vertical + radial	Double vertical
2	Silty fine sand	2 to 8	Radial	Horizontal
3, 4, 5	Silty clayey sand to slightly clayey silty sand	0 to 2	Upwards vertical + radial	Upwards vertical
6	slightly sandy silty clay	1 to 4	Radial	Restricted double vertical
7	slightly silty clayey sand	2 to 5	Horizontal	Horizontal
8	Silty clay	3 to 10	Upwards vertical	Upwards vertical

primary consolidation. This working hypothesis has justified the fact that all settlements measured during the usual period of test embankments monitoring, i.e around a year more or less in most cases, have been considered by them to be entirely primary settlements. This was so since it was judged that primary consolidation had not yet reached its end and, consequently, secondary consolidation had not yet started to occur. The measured settlement curves, mainly the settlement plates curves, were then analyzed using Asaoka's method (Asaoka 1978).

Based on their consideration that for $\overline{U} \geq 33\%$ the series solution of Terzaghi's theory could be replaced by its first term which is:

$$\overline{U} = 1 - 0.811 e^{\frac{-\pi^2}{4} T} \quad (4)$$

it was then considered justifiable to use Asaoka's construction to obtain the total primary settlement and the consolidation coefficient, assuming that a few months after end of construction the average consolidation ratio under field test embankments could be considered to be higher than 33%.

In the case of radial drainage considering equal strain theory, the average consolidation ratio is given by an expression presented by Barron (1948) similar to the one above mentioned, but valid for any value of the consolidation ratio, so that Asaoka's construction could also be applied. In both cases, the consolidation coefficient and total primary settlement thus obtained have been considered sound and trustworthy.

This approach has led to the endlessly repeated conclusion that the back-analyzed field values of the consolidation coefficient are usually about 50 times higher than the laboratory consolidation coefficient and that this fact is totally explained and justified by the existence of providential very thin, obviously continuous, layers of pervious sand. It is worth mentioning that no lense of pervious sand was present in any of the the layer 6 samples.

The authors consider, first, that this explanation is too far-fetched to be acceptable at once and, second, that some basic points could not, and should not, have been overviewed for so many years, as has been the case, by the researchers in the process of reaching the above mentioned published conclusions and, then, of revalidating and republishing them year after year for so long. Some of these points are clearly pointed out by Gonçalves (1992).

The first point which has been systematically overviewed is the fact that the consolidation coefficient values are very different in the range of stresses up to the preconsolidation stress and in the range of stresses beyond the preconsolidation stress. This was very clearly illustrated in Fig. 4 and Bjerrum (1972), just as an example, can be quoted in this respect "The rate of pore pressure dissipation can in principle, be computed on a similar basis as the consolidation settlement, *i.e.* taking into account that the consolidation properties are different in the two ranges, the first one representing the increase in effective stresses in the range from p_0 to p_c and the second one representing the increase in effective stress beyond p_c". This point was clearly brought up by Gonçalves (1992) "It is well known that the c_v value of a preconsolidated soil can be 10 to 100 times higher than the c_v value of a normally consolidated soil. Some papers which compare the behaviours of the soils from Santos lowlands in the field and in the laboratory do not state how the c_v value was obtained and others admit to have used the c_v value corresponding to stresses $\sigma'_v > \sigma'_p$. If in these analysis the c_v value for the preconsolidated range had been used, the differences between field and laboratory behaviours would probably have been smaller".

The second point which has also been systematically overviewed is the fact that much evidence has been brought up in the last decades in the technical literature showing that secondary consolidation under embankments in the field occurs simultaneously with primary consolidation. The argument repeatedly used by the researchers to justify the working hypothesis of secondary consolidation only starting to occur after the end of primary consolidation is based on the fact that since long term settlements measured in the area of Santos vary rather linearly with the logarithm of time, then the formulation "$\Delta e = C\alpha \log \Delta t$" holds true and since $C\alpha$ is historically considered to express the evolution of secondary settlements after primary settlements have ended then the straight line obtained by plotting settlements *vs.* log of time has been taken as being the proof that the working hypothesis is true. Since to the authors it is clear that long field term settlements will vary, for a long period before coming close to stabilization, rather linearly with the logarithm of time, whether they are only primary, or only secondary or the sum of both, the above argument put forward by the researchers is no more than a sophism.

Figure 15 illustrates the traditional working hypothesis which is that the secondary consolidation starts after primary consolidation ends and the alternative working hypothesis which considers that the secondary consolidation and the primary consolidation occur simultaneously.

As clearly indicated on the left side of Fig. 15, with the tradional hypothesis until the end of the primary consolidation, the evolution of strain with time, up to ε_p, is expressed by Terzaghi's consolidation theory which is very familiar to all soils engineers. After the end of the primary consolidation takes place, then the evolution of vertical strain with time is expressed by the traditional formula $\Delta\varepsilon_v = C_{\alpha\varepsilon}\,\Delta \log(t)$ which is also very familiar to all soils engineers.

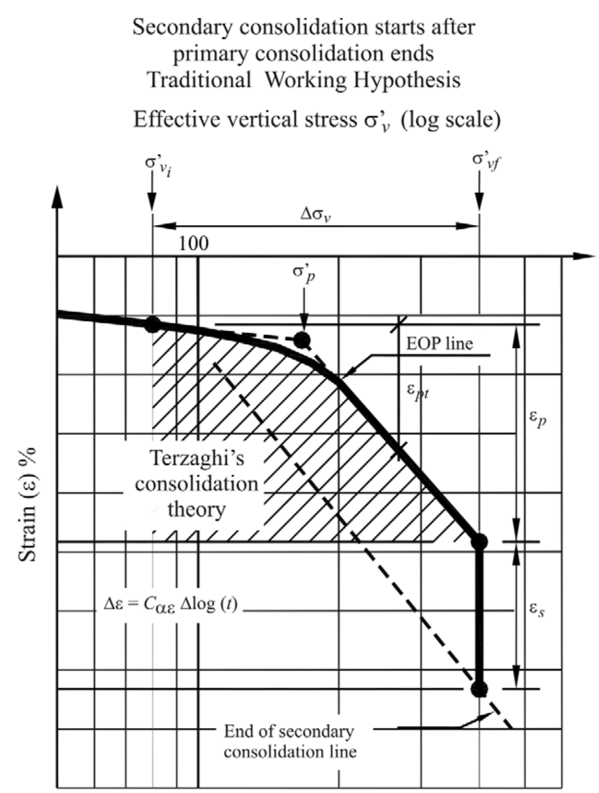

Figure 15 - Traditional and alternative working hypothesis.

The right side of Fig. 15 illustrates the alternative hypothesis which shows that with the primary and secondary consolidations occurring simultaneously, at any time, *t*, the strain is in part due to primary consolidation (ε_{pt}) and in part due to secondary consolidation (ε_{st}). In this case no "of the shelf" functional tool is readily available to calculate the evolution of strain with time, and even if such a tool existed it surely would not be familiar to almost all engineers. In spite of this main drawback of the alternative hypothesis the authors considered, based on the comments presented before, that the only acceptable working hypothesis is the one which considers that primary and secondary consolidations occur simultaneously and decided that this is the one which had to be adopted for their backanalysis, meaning, of course, that the first step to be taken would be to look for and to tailor, if necessary, the tools needed for this task.

10. Working Tool Number 1 to Analyze the Behaviour of the Thick SFL Clay Layer Under Area 3 with Vertical Drainage

A schematic path during field preloading was proposed by Bjerrum (1972) and a schematic path during a controlled gradient oedometer test and during a multiple-stage loading oedometer test were proposed by Leroueil *et al.* (1985). Both propositions are reproduced from the original papers in Fig. 16.

On the left side of Fig. 16, the authors added the values of the "Rate of secondary consolidation", ($\dot{\varepsilon}$) expressed in s^{-1}, calculated from the values per year indicated in Bjerrum's figure. The right side of Fig. 16 shows the figure of the paper by Leroueil *et al.* (1985) corresponding to the multiple stage loading test.

Leroueil *et al.* (1985) stated: "Taylor & Merchant (1940) were the first to suggest a model in which the rate of change in void ratio is a function of the effective stress, the void ratio and the rate of change in effective stress. This suggestion has been followed by numerous researchers. The rheological models proposed were seldom assessed experimentally or only on the basis of a few laboratory test results. Experimental studies, however, have been performed on natural clays and on resedimented clays but in each study only one type of test was used. It is thus difficult to obtain an overall view of the rheological behaviour of clays from these studies. As a result this abundant literature has modified neither the common practice based on the Terzaghi theory nor the way of thinking on clay behaviour". In the authors' knowledge not much has changed from 1985 to 2010, and for sure, practicing engineers continue not disposing of any practical tool to predict or to back-analyze the simultaneous evolution of primary and secondary settlements in soft clayey soils under embankments.

Based on the diagrams shown in Fig. 16 the authors went on to produce their first working tool consisting of an abacus, similar to Bjerrum's but specifically built for the soft clay of layer 6 tested at COPPE, from the laboratory test results. It was expected that this abacus would immediately yield the mean effective stress and mean primary con-

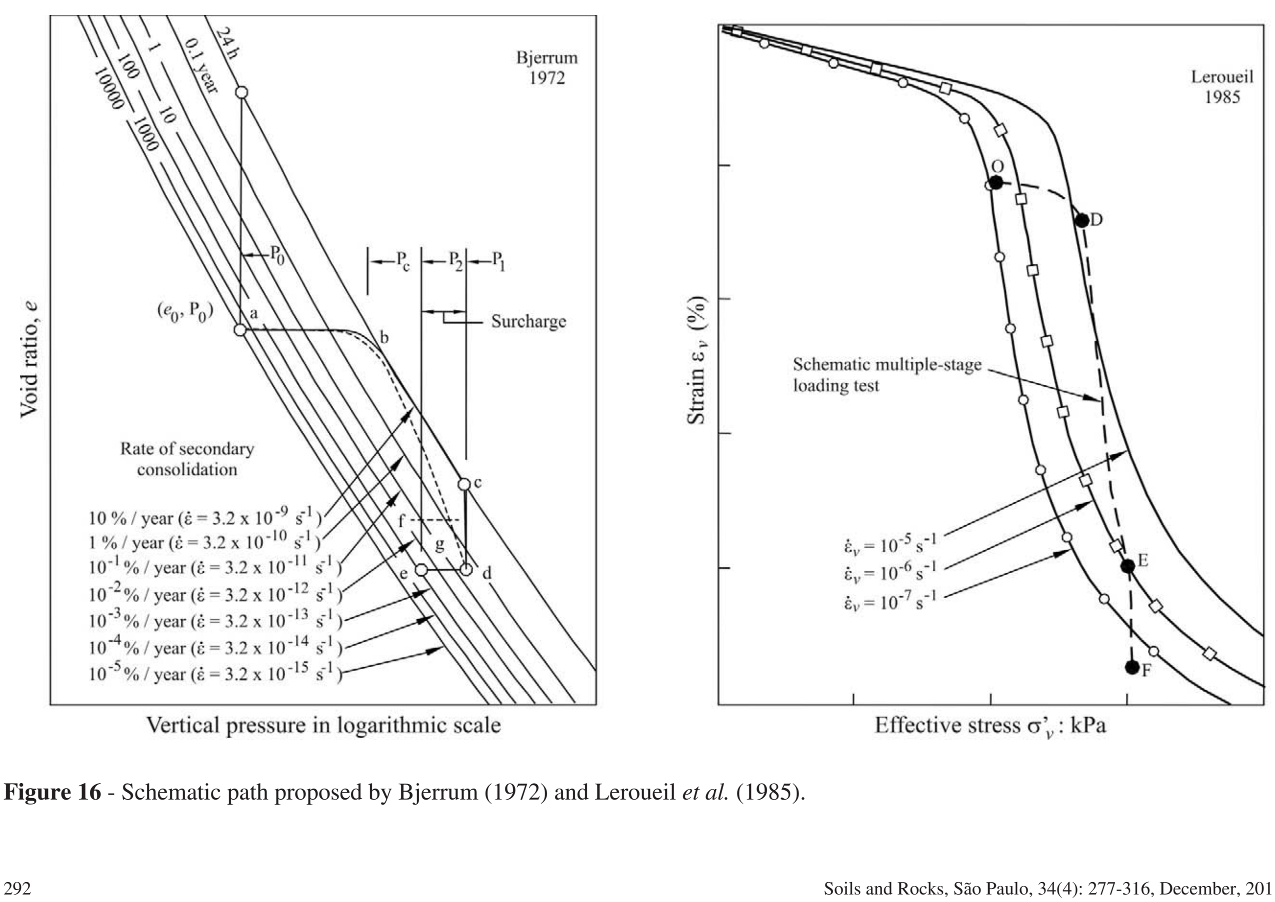

Figure 16 - Schematic path proposed by Bjerrum (1972) and Leroueil *et al.* (1985).

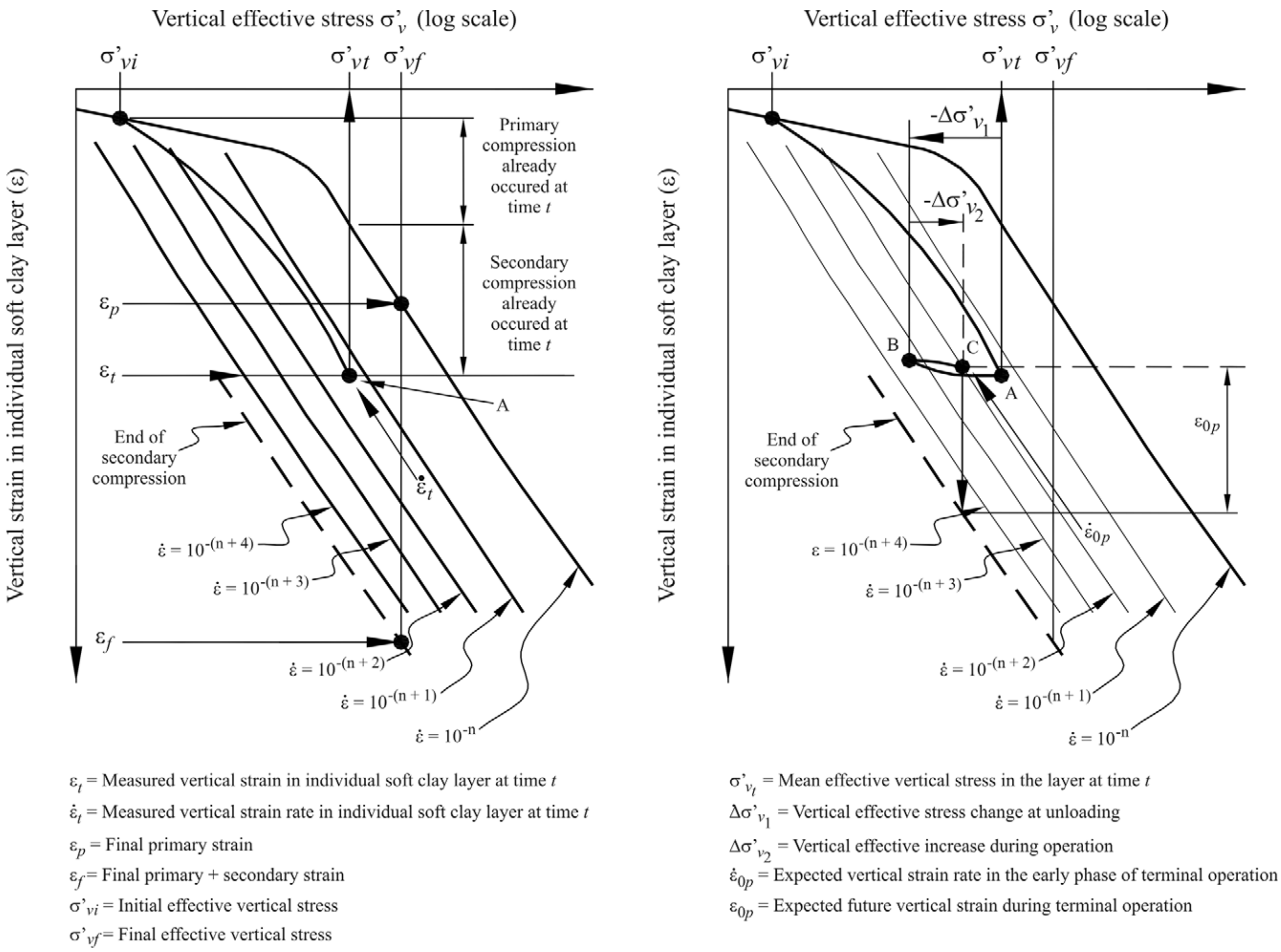

Figure 17 - Methodology expected to be used to analyze layer 6 compression under the pilot embankment.

solidation ratio of layer 6 from the known values of the strain (ε_t) and the strain rate ($\dot{\varepsilon}$) at time *t*. These two values which can be instantly calculated at any time *t* from the layer compression measurements under the pilot embankment would be plotted together on the abacus as illustrated on the left side of Fig. 17 with the strain at time *t* (ε_t) entered in ordinate as a horizontal line extended to the right until it meets the strain rate line representing the value of the strain rate ($\dot{\varepsilon}_t$) occurring in the layer at time *t*, at point A.

From point A, the value of σ'_{vt} = mean effective stress in the layer at time *t* would be directly read in the abacus giving the mean primary consolidation ratio (U_t) at time *t* calculated as

$$U_t = (\sigma'_{vt} - \sigma'_{vi}) / (\sigma'_{vf} - \sigma'_{vi}) \quad (5)$$

It was also expected that the abacus would provide the following informations concerning the future situation during the terminal operation phase that is, after removing the fill surcharge or after stopping applying vacuum in the drains, this resulting in a vertical unloading effective vertical stress change equal to $-\Delta\sigma'_{v1}$, and after terminal operation reaches its normal operation capacity with the application of an effective vertical stress increase $\Delta\sigma'_{v2}$, as illustrated respectively by point B and by point C on the right side of Fig. 17:

$\dot{\varepsilon}_{0p}$ = the expected vertical strain rate in the early phase of terminal operation and

ε_{0p} = the expected vertical strain left to occur during the terminal life.

From these two values, not only of layer 6, but also of all other layers, then the expected rate of settlement of the terminal pavement, in cm per month, at the beginning of normal operation and the total remaining settlement to occur and consequent expected frequency of maintenance operations and total volume of fill to be used to keep levelling the pavement to its nominal elevation during the life of the terminal could be quantified.

The special oedometer tests mentioned in item 5 were programmed to provide the necessary information to produce this type of abacus representative of the behaviour of layer 6. Figure 18 shows on the left side the results of all special oedometer tests which provided strain rates determination during secondary consolidation plotted as log of strain rate (log $\dot{\varepsilon}$ in s^{-1}) *vs.* overconsolidation ratio (OCR). The curve of the left side of Fig. 18 was used, together with the compressibility curve of sample SRA-203(4) to produce the abacus on the right side.

As shown in Table 5, in area 3, in October 2009, the measured strain in layer 6 was 1.9% and the strain rate was 1.2 x 10^{-10} s^{-1}. As can be seen on the right side of Fig. 18, the strain rate value plots very close to the line which represents the end of secondary compression on the abacus, obviously a nonsense since the consolidation ratio of layer 6 under area 3 is, without any doubt, very low as shown by its small measured compression equal to 18 cm when compared to the 90 cm of measured compression at the same time under area 1 as reported in Table 5.

This indicates that the abacus of Fig. 18 is only representative of the behaviour of a 2 cm thick sample of layer 6 soft clay and that for any given clay, there exists a different specific abacus which represents the behaviour of the clay, for each layer thickness.

The question which then arose is "can the abacus for layer 6 be obtained through some realistic model from the laboratory sample abacus of Fig. 18?"

11. Working Tool Number 2 to Analyze the Behaviour of the Thick SFL Clay Layer Under Area 3 with Vertical Drainage

Following this ill success with working tool number 1, the authors then decided to go for an abacus of the same type, but built specifically for the field conditions through extrapolating the abacus shown on the right side of Fig. 18 from the laboratory conditions to the field conditions by way of Taylor and Merchant's formulation as shown below.

As mentioned by Leroueil *et al.* (1985), many formulations have been put forward to try and model secondary consolidation occurring together with primary consolidation and Taylor and Merchant's theory (theory A) was the first one published in the technical literature stating a basic postulate to express the evolution of the soil void ratio with time during secondary consolidation. This postulate is illustrated at the top of Fig. 19 and its basic formulation is:

$$\frac{\partial e}{\partial t} = -\mu(\overline{cd}) \tag{6}$$

which states "that the speed of occurrence of secondary compression is proportional to the undeveloped secondary compression" where μ is called the "coefficient of secondary compression". The mathematical solution to compute the "aggregate consolidation ratio" based on the above postulate was given by Taylor & Merchant (1940) in their paper and it shows that the evolution of this ratio depends on the two following parameters:

• *r* which is the ratio of the primary settlement over the total settlement, showing that Taylor and Merchant had a clear understanding that secondary compression was finite and could be estimated and

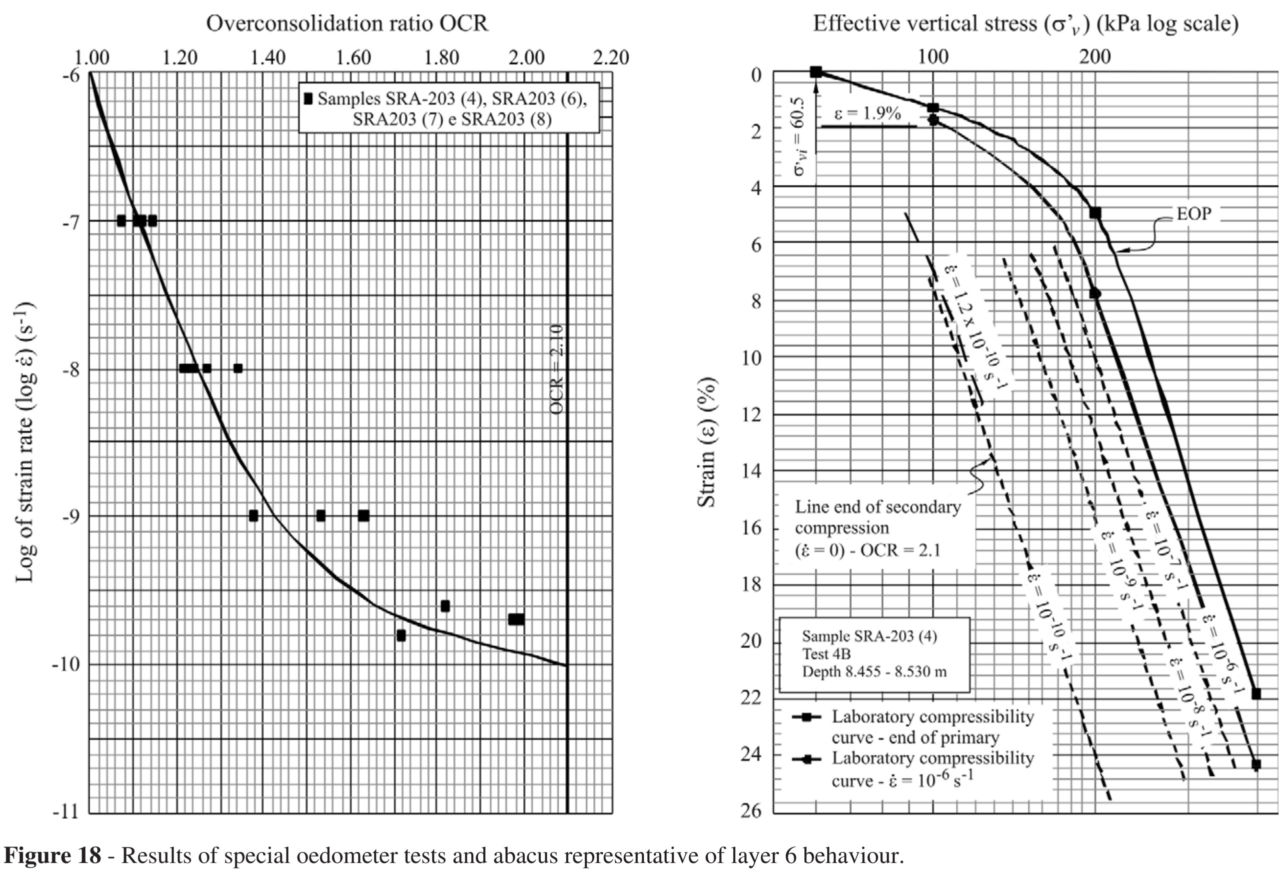

Figure 18 - Results of special oedometer tests and abacus representative of layer 6 behaviour.

- $F = \dfrac{\mu t}{rT} = \dfrac{\mu H_d^2}{r c_v}$ (7)

a dimensionless term called the "secondary compression factor".

The original paper includes a graph showing the aggregate consolidation ratio where it can be appreciated that this is the ratio of the settlement (or compression or strain) at time *t* over the total (primary plus secondary) settlement (or compression or strain) plotted as a function of the time factor *T* for the case of unidimensional vertical compression with only vertical drainage for an *r* value of 0.70 and for various values of the *F* factor which are reproduced as non dotted curves at the bottom of Fig. 19. The aggregate consolidation ratio will be referred to as U_{p+s}. In Taylor and Merchant's own words, this formulation is "based largely on physical intuition" and "the main value of this theory is not in the expression of a secondary compression time law, but in the rational explanation of the superimposed action of the two very different physical laws of time rate, allowing the prediction of the action in thick strata from the action in laboratory tests". This "prediction of the action in thick strata from the action in laboratory tests" is the way to extrapolate the abacus shown on the right side of Fig. 18 from the laboratory conditions to the field conditions by way of Taylor and Merchant's formulation as shown below which the authors decided to use to build their working tool number 2. Of course, the field abacus would be used in the same way as working tool number 1, that is determining the mean effective stress and mean primary consolidation ratio of layer 6 from the known values of strain and strain rate at time *t*.

It has been shown by Christie (1964) that the formulas published in Taylor and Merchant's paper are mistaken, but that their curves which are reproduced at the bottom of Fig. 19 are in accordance with the correct formulas reestablished by Christie (1964) in terms of excess pore pressure. Furthermore, Christie (1964) showed that Gibson & Lo's (1961) formulation is identical to Taylor and Merchant's although expressed in different terms. The mathematical formulation for Taylor and Merchant's theory has also been obtained by Carvalho (1997) in terms of void ratio. Carvalho's formulas were used by the authors to compute the aggregate consolidation ratio for *r* = 0.70 and *F* values of 0, 0.1 and 10 obtaining perfect agreement with Taylor and Merchant's curves as seen on Fig. 19. All further calculations performed using Taylor and Merchant's theory included ahead in this paper were done using Carvalho's formulas.

A number of long term oedometer tests has been performed in the laboratory of the Rheology Group of the Soil Mechanics Division at COPPE, Rio de Janeiro as shown in Figs. 20, 21 and 22.

Figures 20, 21 and 22 show the measured laboratory curves and the theoretical curves obtained from Taylor and Merchant's theory which best fit the experimental curves for two soft clay samples of the Rio de Janeiro area, Senac clay (Martins 2005) and Sarapuí clay (Vieira 1988) and for a specimen trimmed from a sample prepared through a mixture of kaolin (90%) and bentonite (10%) (Martins 2005), respectively. Line AB shows for each test the line from which the value of the coefficient of secondary consolidation $C\alpha$ would be normally determined from the oedometer test result. As can be seen this line only fits the test results up to $t = 10^5$ min, that is about 70 days, after that a much higher value of $C\alpha$ would be required to fit the test results.

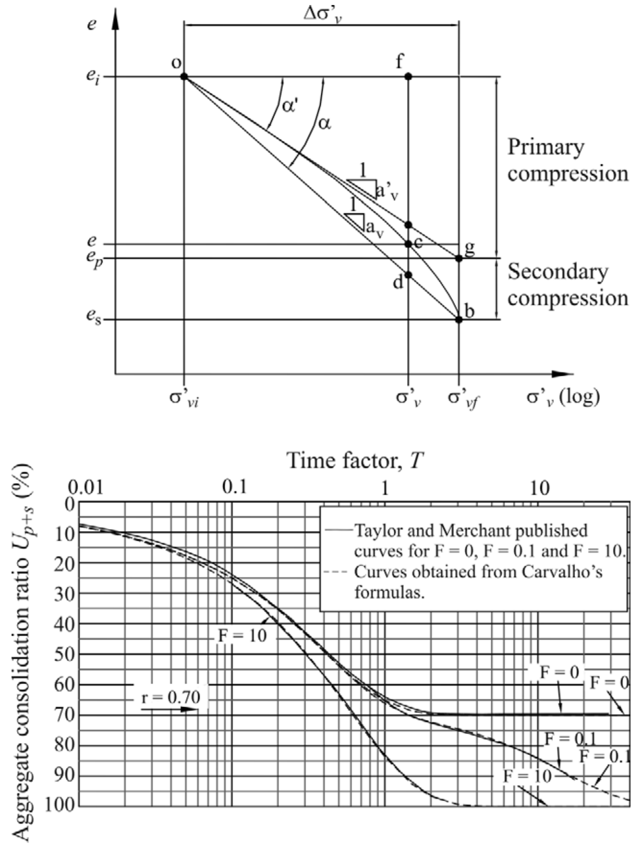

Figure 19 - Taylor and Merchant's theory (Theory A) basic postulate and aggregate consolidation curves.

The best fit is obtained by varying the three parameters: *r*, c_v and μ and each diagram on Figs. 20, 21 and 22 shows the values which provided the best fit in each case. The values, which are only valid for the given range of stresses applied on the tested samples and not for the clay deposit as a whole, are compared in Table 10.

The longest of the 3 tests is the one on the Senac clay, illustrated in Fig. 21, which lasted for 5 years and it can be seen that for the last 19 months, that is after 3.4 years up to 5 years, the compression was totally stabilized, confirming that the secondary compression is finite and that it completely stabilizes within a given time. As can be seen on all three diagrams, the Taylor and Merchant's theory agrees rather well with the experimental curves at the beginning

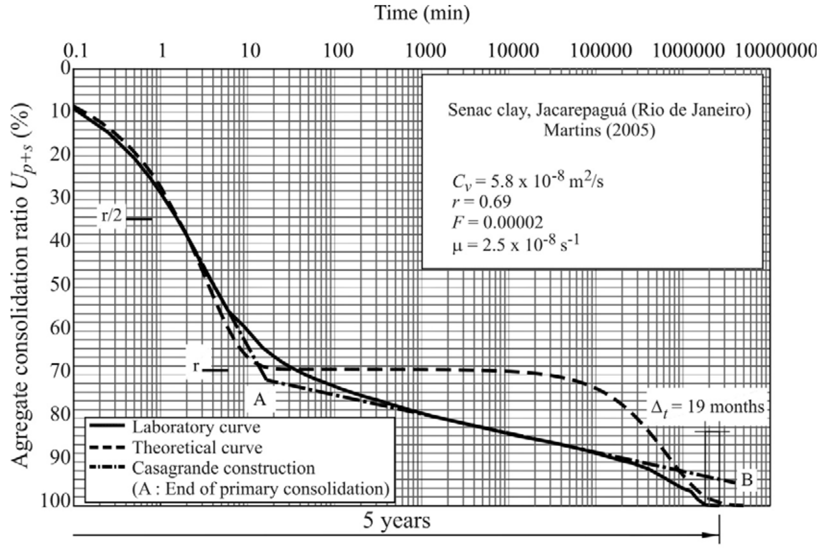

Figure 20 - Comparison of long term oedometer test in Senac clay with Taylor and Merchant's theory.

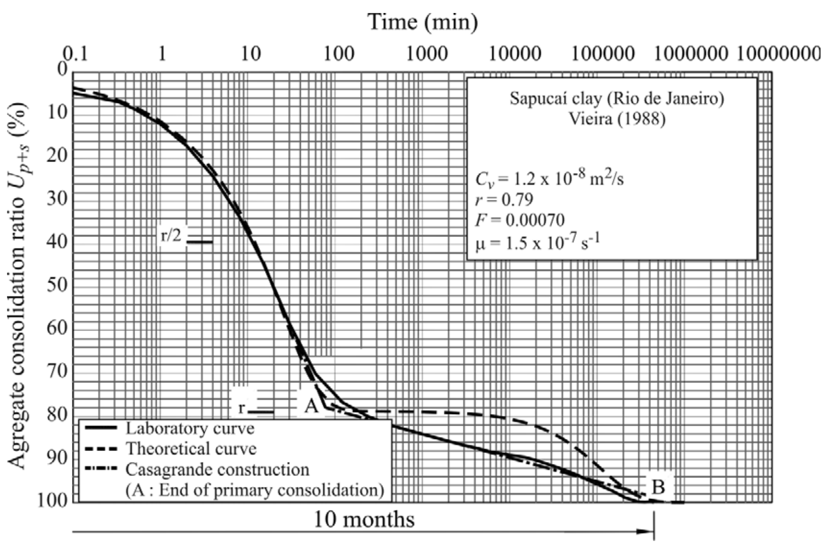

Figure 21 - Comparison of long term oedometer test in Sarapui clay with Taylor and Merchant's theory.

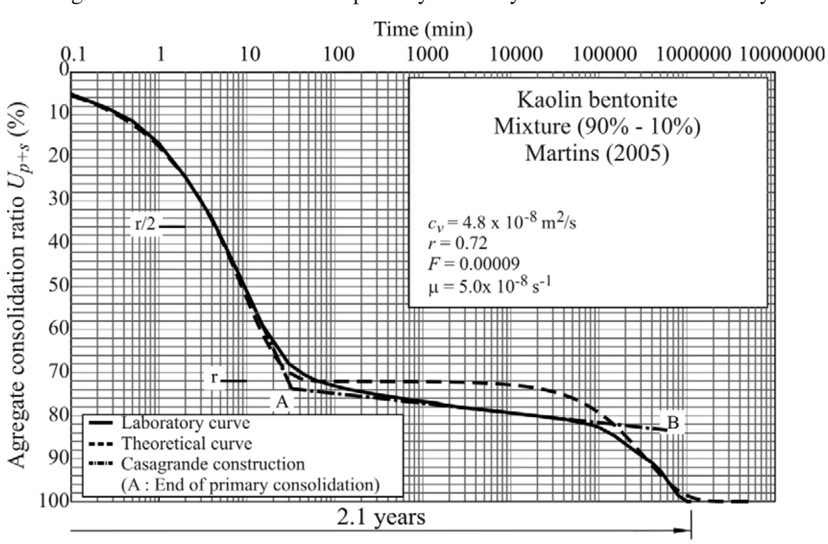

Figure 22 - Comparison of long term oedometer test in a kaolin-bentonite mixture with Taylor and Merchant's theory.

Table 10 - Values of r, c_v and μ for Senac clay, Sarapuí clay and kaolin-bentonite mixture.

	Senac clay	Sarapuí clay	Kaolin + bentonite
r	0.69	0.79	0.72
c_v (10^{-8} m^2/s)	5.8	1.2	4.8
μ (10^{-7} s^{-1})	0.25	1.5	0.5

and at the end of the consolidation process but fails to provide good agreement in between, where it can be seen that the measured secondary compression is consistently higher than the theoretically predicted one, which means, in other words, that the secondary consolidation on 2 cm thick samples proceeds faster than modeled by Taylor and Merchant's theory mainly in the middle of the process.

Figure 23 shows Taylor and Merchant's aggregate consolidation ratio U_{p+s} *vs.* time factor T for samples or clay layers, double drained (H_d = drainage distance = half the thickness) with thicknesses of 20 mm (lab sample), 40 mm, 80 mm, 200 mm, 1 m, 4 m and 20 m for a clay with $c_v = 1.0 \times 10^{-8}$ m^2/s, $\mu = 1.5 \times 10^{-7}$ s^{-1} and with $r = 0.30$.

Figure 24 shows Taylor and Merchant's aggregate consolidation ratio U_{p+s} *vs.* time t for samples or clay layers, double drained (H_d = drainage distance = half the thickness) with thicknesses of 20 mm (lab sample), 40 mm, 80 mm, 200 mm, 1 m, 4 m and 20 m for a clay with $c_v = 1 \times 10^{-8}$ m^2/s, $\mu = 1.5 \times 10^{-7}$ s^{-1} and with $r = 0.30$.

Line AB drawn on Fig. 24 for H_d = 10 mm, that is for the standard oedometer test, is the line from which the value of the coefficient of secondary consolidation $C\alpha$ would normally be determined from the laboratory consolidation curve plotted in terms of Δe *vs.* log (t). According to Taylor and Merchant's formulation, it can be seen that the inclinations of the lines drawn in Fig. 24 for clay thickesses up to

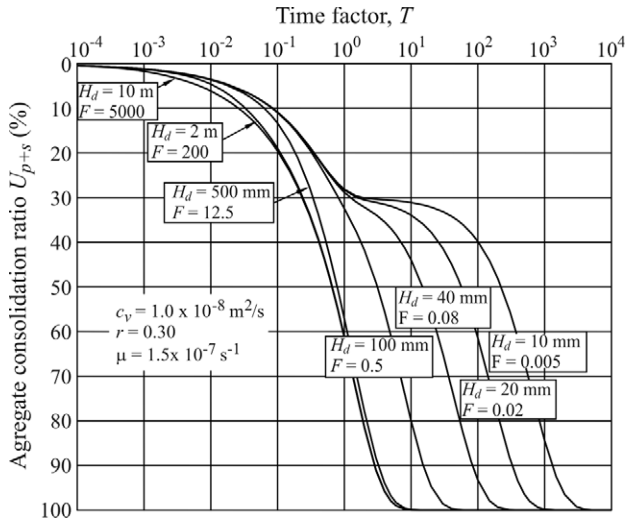

Figure 23 - Taylor and Merchant's curves: Aggregate consolidation ratio U_{p+s} *vs.* time factor T.

200 mm, that is for H_d up to 100 mm, in the range $U_{primary}$ > 90%, that is below the black point marked on each curve, would not be constant through time, as already observed on the actual laboratory tests curves shown in Figs. 20, 21 and 22. It can also be seen that the inclinations of all the curves in the range $U_{primary}$ > 90% are about the same for H_d between 500 mm and 10 m: 1:69 to 1:66, and it is clear that these inclinations are totally different from the laboratory $C\alpha$ line which is 1:1.1.

Table 11 shows the time to reach U_{p+s} equal to 99.9% from Taylor and Merchant's theory in a clay with $\mu = 1.5 \times 10^{-7}$ s^{-1} and $r = 0.3$.

It seems reasonable to expect that for any thickness, Taylor and Merchant's theoretical curves might be rather realistic at the beginning and at the end of the consolidation

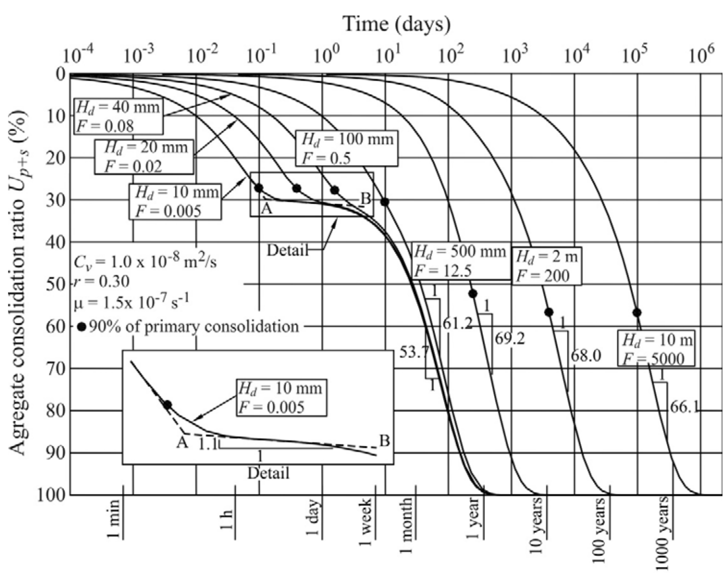

Figure 24 - Taylor and Merchant's curves: Aggregate consolidation ratio U_{p+s} *vs.* time t.

Table 11 - Time to reach U_{p+s} equal to 99.9% from Taylor and Merchant's theory in a clay with $\mu = 1.5 \times 10^{-7}$ s^{-1} and $r = 0.3$.

c_v (m^2/s)	Thickness (H) of double drained layer				
	2 cm	20 cm	2 m	10 m	20 m
4×10^{-7}	500 days 1.37 year	500 days 1.37 year	500 days 1.37 year	4000 days 11.0 years	15 000 days 41.1 years
10^{-8}	500 days 1.37 year	500 days 1.37 year	6000 days 16.4 years	150 000 days 411 years	600 000 days 1644 years

process and might underestimate the settlement (or strain) in the middle of the process as was observed on the 2 cm thick laboratory samples (see Figs. 20, 21 and 22). As a consequence, it might then be admitted that for all predictions based on Taylor and Merchant's theory with reliable soil parameters, with emphasis on a realistic value of c_v corresponding to the range of effective vertical stress (σ'_{vi} to σ'_{vf}) effectively applied, not a simple task when $\sigma'_{vi} < \sigma'_p < \sigma'_{vf}$, the real value of secondary compression will always be equal to or higher than the predicted one mainly in the middle of the process.

With this limitation in mind, the authors proceeded to build the abacus for the field conditions of layer 6 under the center of area 3 using Carvalho's formulas for the specific values of:

• Layer thickness = 9.50 m, vertically double drained with no restriction, although Table 9 indicates that drainage conditions of layer 6 is considered to be "Restricted double vertical",

• $C_c/(1 + e_0) = 0.56$ and $C_r/(1 + e_0) = 0.11 \times C_c/(1 + e_0) = 0.062$,

• $\sigma'_{vi} = 82$ kPa, $\Delta\sigma'_v = 78$ kPa and $\sigma'_{vf} = 160$ kPa,

• $\sigma'_p = 187$ kPa,

• $c_v = 1.5 \times 10^{-8}$ m^2/s and

• $\mu = 1.5 \times 10^{-7}$ s^{-1} (this value is the only one which has not been experimentally determined specifically for the clay of layer 6 since, to the authors' knowledge, the only way to determine the μ value is from long term oedometer tests run till the end of secondary consolidation, that is for at least 10 months as in the case of Sarapui clay shown in Fig. 21 to more than 41 months as in case of Senac clay shown in Fig. 20 through the adjustment of Taylor and Merchant's theoretical curves to the experimental curves. The value of μ which was used is the one of Sarapui clay.

The abacus thus obtained is shown on Fig. 25.

In this abacus, point P corresponds to the initial state of the middle of layer 6 before building the pilot embankment, that is with an initial vertical effective stress equal to 82 kPa and a strain ε' relative to its initial state obviously equal to zero. The preconsolidation stress in the middle of layer 6 is 187 kPa which corresponds to an OCR value a little higher than the value of 2.1 which would be equivalent to the end of secondary consolidation. This means that during consolidation under an applied load, layer 6 primary compression would plot on the primary recompression line PQ for σ'_v smaller than σ'_p. In october 2009, the measured mean strain in layer 6 was 1.9%, represented as ε' and the measured strain rate in layer 6 was $\dot{\varepsilon} = 1.2 \times 10^{-10}$ s^{-1} (as shown in Table 5) which would correspond to point Q in the abacus. As can be seen, point Q would correspond to an applied effective stress of 142 kPa which would mean an average primary consolidation ratio equal to (142-82)/(160-82) = 77%. This does not suit the experimental measured settlement data which, as already mentioned indicates that the consolidation ratio of layer 6 under area 3 is, without any doubt, very low as shown by its small measured compression equal to 18 cm when compared to the 90 cm of measured compression at the same time under area 1 as reported in Table 5. Point A is very close to the recompression line, in the heart of the recompression range. Since the c_v value which governs primary consolidation in the recompression range is roughly 50 times higher than the c_v value of 1.5×10^{-8} m^2/s of the virgin compression range used to build the abacus (see Fig. 4), it cannot be expected that the abacus shown in Fig. 25 yield worthy results.

The abacus was then rebuilt, using the same procedure but using the c_v value of the recompression range equal to 10^{-6} m^2/s but this also failed to lead to acceptable results. The authors had then to come to the conclusion that their second working tool consisting in an abacus tailored to represent the field conditions of layer 6 through extrapolation of the abacus built from the oedometer laboratory test results by way of Taylor and Merchant theory also failed to be usable, the main reason for this being that the c_v value in the field varies when the consolidation ratio increases, as will be seen in the conclusions, and that Taylor and Merchant's formulation used to built the abacus only allows the use of a constant c_v value.

12. Working Tool Number 3 to Back-Analyze the Behaviour of the Thick SFL Clay Layer Under Area 3 with Vertical Drainage

After coming to this conclusion, the authors found themselves left with only one alternative to back-analyze the measured compression in layer 6 under the center of area 3, and that was to try and adjust some Taylor and Merchant's curve to the measured curve of Fig. 11 determining the c_v value which would lead to a reasonable adjustment. As already mentioned, as settlement occurs, the total stress

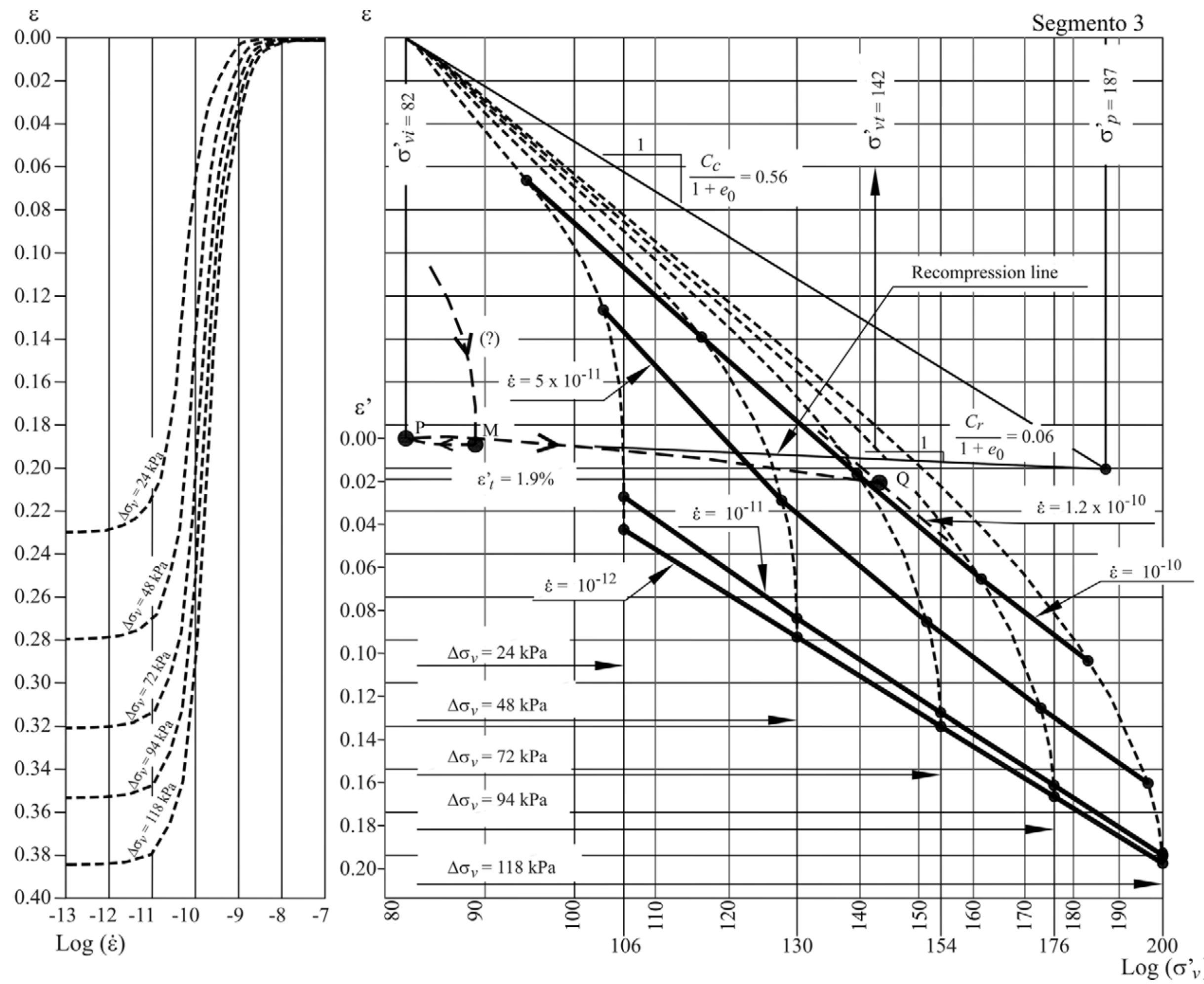

Figure 25 - Abacus built through Taylor and Merchant's theory for layer 6 of area 3 with $c_v = 1.5 \times 10^{-8}$ m²/s.

σ_v in the middle of layer 6 decreases with time due to embankment submersion and the "pseudo final effective stress" which governs the consolidation process at any time, that is "σ_v - u_{hid}", also decreases as illustrated in Fig. 26. For their back-analysis, the authors took the decision to calculate the values of "σ_v - u_{hid}" acting in october 2009 in each of the 1 m thick sublayers considered for settlement calculations.

The "pseudo final effective stress" at mid-height of layer 6, "σ_v - u_{hid}" is equal to 179.2 kPa compared to σ'_{vi} = 81.4 kPa and σ'_p (lab) = 187.3 kPa and is, in fact, higher than the (real) final effective stress, equal to 160.6 kPa, to be reached after full primary and full secondary consolidations when the total settlement will be 2.89 m wheras the total settlement at the end of october 2009 was 1.01 m.

The primary and secondary compressions were then calculated considering that this "pseudo final effective stress" would be maintained constant thereafter, obtaining:

• "pseudo final primary compression" (ΔH_p)': 20 cm which is, in fact, higher than the (real) final primary compression to be reached after full primary consolidation which is equal to 18 cm as indicated in Table 8.

• "pseudo final secondary compression" (ΔH_s)': 142 cm which is, in fact, higher than the (real) final secondary compression to be reached after full secondary consolidation which is equal to 120 cm as indicated in Table 8 and their sum:

• the "pseudo final total compression" (ΔH_t)': 162 cm which is, in fact, higher than the (real) final total compression to be reached after full primary and full secondary consolidations which is equal to 138 cm.

It was immediately found out that no satisfying adjustment was to be obtained with only one constant value of c_v over the whole period. Figure 27 shows a theoretical Taylor and Merchant's curve reasonably well fitted to the measured compression curve of layer 6 under the center of area 3.

This adjustment was achieved by dividing the total measurement period into three periods. As can be seen on Fig. 27, the values of c_v which led to the adjustment of the theoretical curve to the measured one are:

• for the first period: $c_v = 2 \times 10^{-7}$ m²/s,

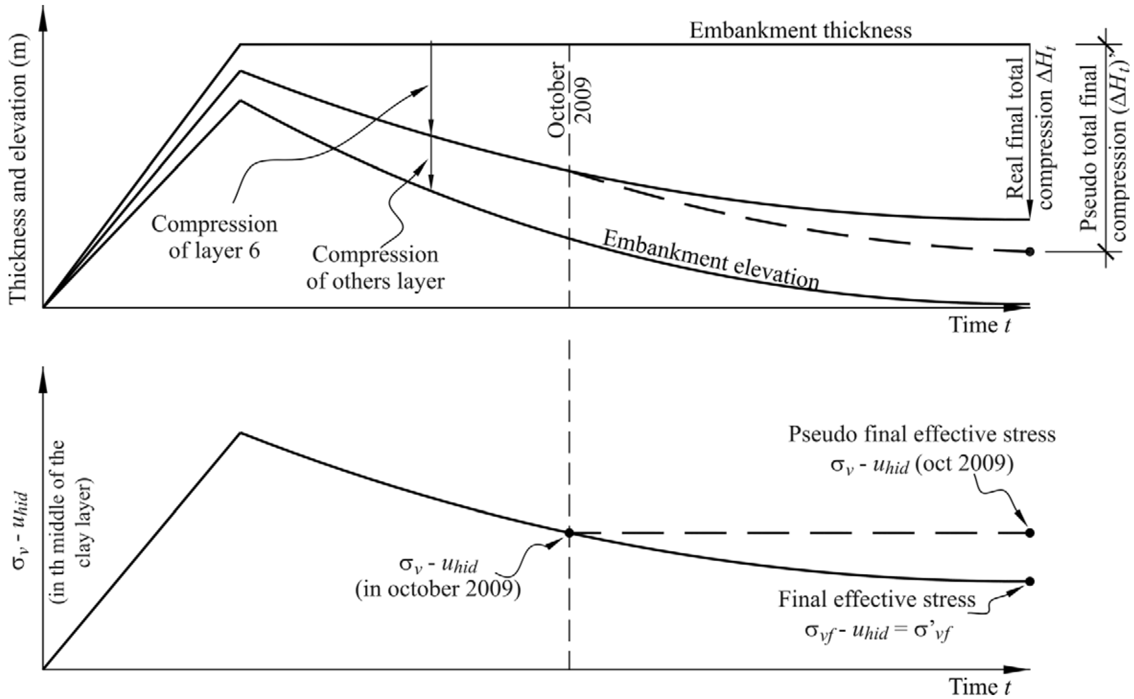

Figure 26 - Evolution of the "pseudo final effective stress" in the middle of layer 6 and of the "pseudo total final compression".

• for the second period: $c_v = 5 \times 10^{-8}$ m^2/s,

• for the third period: $c_v = 1 \times 10^{-8}$ m^2/s

Table 12 summarizes the results of the back-analysis of layer 6 compression with vertical drainage under the center of area 3 through Taylor and Merchant's theory, indicating:

• the equivalent time of the end of each period,

• the coefficient of consolidation for which the best fit was obtained between the theoretical curve and the measured compression curve, in each period: c_v during period 1, c_v during period 2, c_v during period 3,

• the total compression ΔH_{tj} measured at the end of each period,

• the calculated primary compression, ΔH_{pj}, and secondary compression, ΔH_{sj}, at the end of period 1, period 2 and period 3,

• the calculated ratio of the primary compression at the end of each period ΔH_{pj} to the "pseudo final primary compression" (ΔH_p)' called the "primary consolidation index",

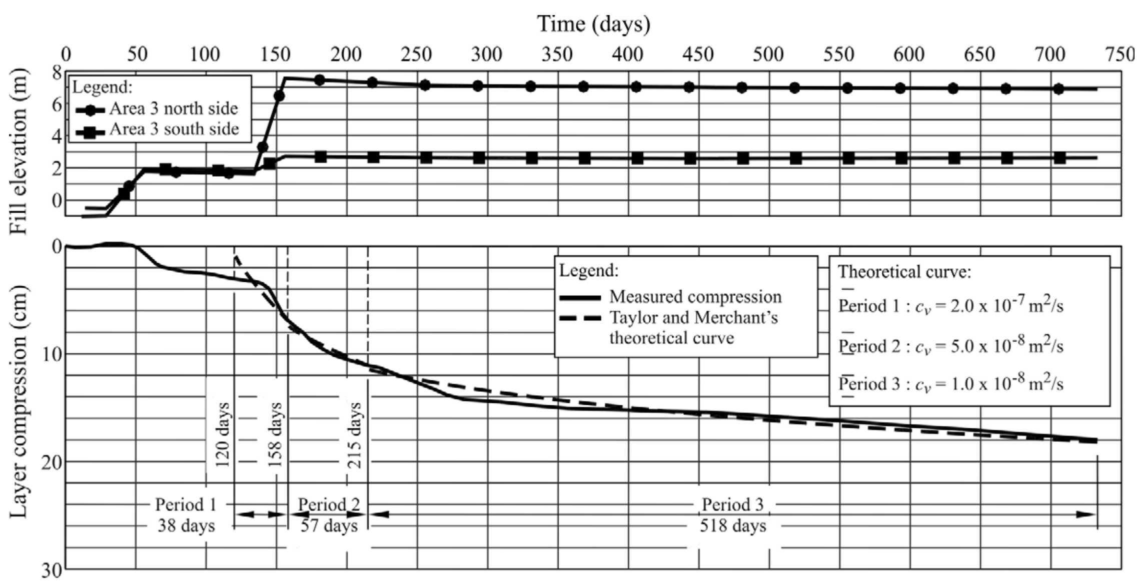

Figure 27 - Theoretical Taylor and Merchant's curve reasonably well fitted to the measured compression curve of layer 6 under the center of area 3.

Table 12 - Results of the back analysis of layer 6 compression under the center of area 3.

	Period 1	Period 2	Period 3
Time *t* (equivalent) at the end of each period	38 days	95 days	613 days
Back analyzed c_v value for each period	20 x 10^{-8} m^2/s	5.0 x 10^{-8} m^2/s	1.0 x 10^{-8} m^2/s
ΔH_{tj}: Total compression of layer 6 measured at the end of each period	7 cm	11 cm	18 cm
ΔH_{pj} compression at the end of each period obtained from Taylor and Merchant calculations	4 cm	6 cm	8 cm
$\Delta H_{pj}/(\Delta H_p)$' Primary consolidation index at the end of each period	4/20 = 20%	6/20 = 30%	8/20 = 40%
ΔH_{sj} compression at the end of each period obtained from Taylor and Merchant calculations	3 cm	5 cm	10 cm
$\Delta H_{sj}/(\Delta H_s)$' Secondary consolidation index at the end of each period	3/142 = 2.1%	5/142 = 3.5%	10/142 = 7.0%
$\Delta H_{tj}/(\Delta H_t)$' Aggregate consolidation index at the end of each period	7/162 = 4.3%	11/162 = 6.8%	18/162 = 11.1%

• the calculated ratio of the secondary compression at the end of each period ΔH_{sj} to the "pseudo final secondary compression" (ΔH_s)' called the "secondary consolidation index",

• the calculated ratio of the total compression at the end of each period ΔH_{tj} to the "pseudo final total compression" (ΔH_t)' called the "aggregate consolidation index".

It has to be emphasized that when secondary compression and primary compression occur simultaneously, the volume of water expelled in this situation is larger than the volume of water which would be expelled if only primary consolidation took place. Since the initial pore pressure and the initial gradient are not affected by the phenomenon of secondary consolidation, then the pore pressure dissipation has to be slower when secondary consolidation occurs simultaneously with primary consolidation than if it did not as illustrated in Fig. 28.

This fact has been pointed out by Garlanger (1971) among others. Larsson *et al.* (1997) can be quoted: "At compression, the time dependence leads to a larger compression than that calculated from the compression moduli alone. A condition for this extra compression to occur is that the corresponding amount of water flows out of the soil. In turn, a condition for this to occur within the same period of time as the compression corresponding to the moduli alone is that a higher gradient exists in the pore water. The immediate effect of the creep tendency (or time effects) during a short time step is therefore an increase in pore pressure, whose size is determined by the pontential creep deformation and the compression modulus". This is illustrated on the left side of Fig. 28. The right side of Fig. 28, shows the comparison of the measured settlement of an embankment on soft clay with Larsson *et al.*'s prediction. Taylor and Merchant's theory, although only stated in terms of void ratio, does not take into account the influence of the occurrence of secondary compression simultaneously with primary compression on the pore pressure, as clearly shown by Carvalho's formulas, but this influence will necessarily lead to a field c_v value lower than the laboratory pure primary consolidation c_v value as clearly illustrated at the top of the left side of Fig. 28.

It can be assumed that the value of the average primary consolidation ratio $\overline{U}_p$ is equal to the primary consolidation index $[\Delta H_{pj}/(\Delta H_p)']$, so that the average vertical effective stress in layer 6 at the end of each period can be computed from the following formula:

$$\sigma'_v = \sigma'_{vi} + [(\sigma_v - u_{hid}) - \sigma'_{vi}] \times \overline{U}_p = \sigma'_{vi} + [(\sigma_v - u_{hid}) - \sigma'_{vi}] \times [\Delta H_{pj} / (\Delta H_p)'] \qquad (8)$$

allowing then, to plot the back-analyzed values of c_v against the mean effective vertical stress σ'_v in layer 6 in area 3, as shown in Fig. 29.

It is well known that the yielding stress decreases when the strain rate decreases as illustrated in Fig. 16. It has, therefore, to be expected that the vertical effective stress at which the field c_v value passes from its higher value, between 3 x 10^{-6} m^2/s and 3 x 10^{-7} m^2/s (see Fig. 4) in the recompression range, to its lower value, between 9 x 10^{-9} m^2/s and 2 x 10^{-8} m^2/s (see Fig. 4) in the virgin compression range, is to be smaller than the σ'_p value determined in the oedometer tests.

It can be seen in Fig. 29 that the obtained results are in good agreement with the above observation and that the back-analyzed c_v field values are also in good agreement with the laboratory values in the transition range between the recompression range and the virgin compression range.

13. Working Tool Number 4 to Extrapolate the Use of the Taylor & Merchant Model to Back-Analyze the Behaviour of the Thick SFL Clay Layer Under Areas 1 and 2 with Radial Drainage

13.1. Methodology

For the back-analysis of the embankment settlement data for layer 6 under the centers of areas 1 and 2 the same approach is not applicable due to the fact that the mathe-

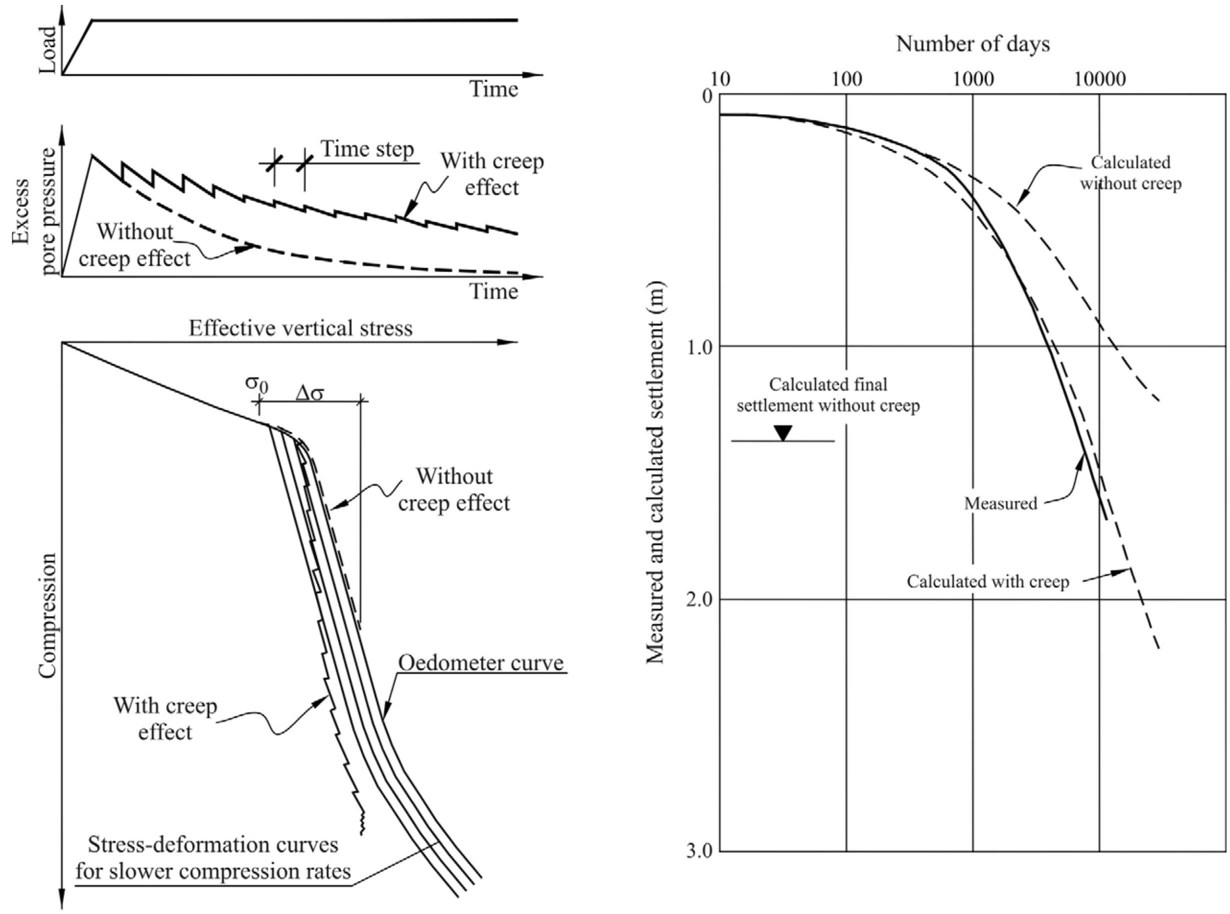

Figure 28 - Influence of the occurrence of secondary compression simultaneously with primary compression apud Larsson *et al.* (1997).

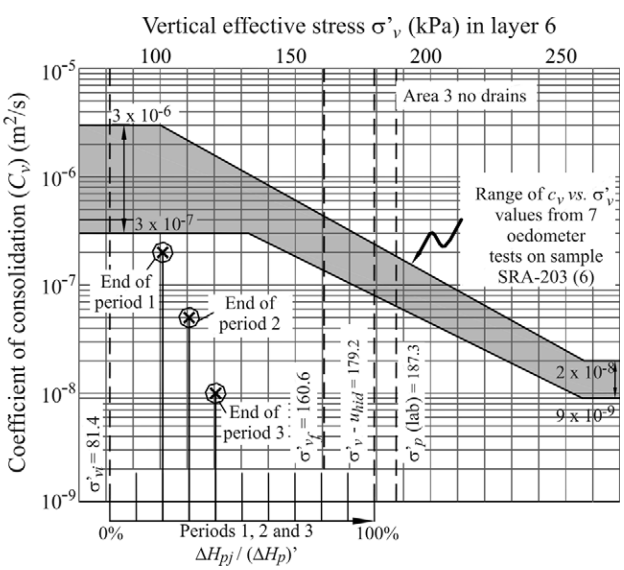

Figure 29 - Back-analyzed values of c_v *vs.* mean effective vertical stress in layer 6 under area 3.

matical formulation presently available based on Taylor and Merchant's theory only encompasses the case of vertical drainage. In this respect, the authors are not aware of any published analytical formulation of secondary consolidation associated with radial drainage.

It was then decided to compare the primary consolidation process of layer 6 undergoing vertical compression through pure radial drainage with a mean radial drainage distance R equal to 0.68 m which corresponds to the drain spacing of 1.2 m of the square wick drains mesh under area 1, to the primary consolidation process of a hypothetical layer undergoing vertical compression with pure vertical drainage to see if a layer such that both processes would follow approximately the same course could be found.

As can be seen in Table 3, for layer 6 the value of c_{h1} determined from CPT porepressure dissipation tests, which corresponds to the recompression range according to Teh and Houlsby (1991), is equal to 4.9 x 10^{-7} m^2/s and the oedometer test c_{v1} value in the recompression range is 6.5 x 10^{-7} m^2/s, that is $c_{h1} = 0.75\ c_{v1}$. Some oedometer tests with radial drainage were performed in the laboratory which yielded c_h values of the order of 3 times the c_v values in the normal compression range. For this reason, all further calculations were done for $c_h = c_v$ as well as for $c_h = 3\ c_v$.

For this comparison, the radial primary consolidation process of layer 6 was calculated using Barron (1948) formulas considering an equivalent radius r_w of 3.25 cm for the

0.5 cm x 10 cm wick drain and a smear zone around each drain with a radius r_s equal to twice the drain equivalent radius, and a permeability coefficient equal to a fifth of the undisturbed clay permeability coefficient. Figure 30 shows the dotted curve which expresses the (primary) consolidation ratio of layer 6 under area 1 *vs.* the logarithm of time calculated for a horizontal/radial coefficient of consolidation $c_h = 1.5 \times 10^{-8}$ m^2/s.

Figure 30 also shows the plain curve which corresponds to a hypothetical layer with vertical drainage, with the primary consolidation ratio calculated using Terzaghi (1936) formulation considering $c_v = 1.5 \times 10^{-8}$ m^2/s and the drainage distance D equal to 2.03 m for which the two curves reach $U = 50\%$ at the same time. Considering the closeness of the two curves, it can be concluded that this layer undergoing vertical compression with pure vertical drainage follows a primary consolidation process equivalent to the one of layer 6 under area 1 undergoing vertical compression through pure radial drainage and the D value of 2.03 m can be called the equivalent drainage distance: D_{eq}.

The equivalent drainage distance value is influenced by the ratio of the value of c_h of layer 6 to the assumed value of c_v of the equivalent layer with vertical drainage. It is also influenced by the assumed values of the radius and the coefficient of permeability of the smear zone. For this reason, the D_{eq} value was also determined for c_h/c_v equal to 3 and for a smear zone three times larger than the one considered before, that is with r_s = 19.5 cm.

The D_{eq} value was also determined following exactly the same methodology explained above for layer 6 undergoing vertical compression through pure radial drainage with a mean radial drainage distance R equal to 1.35 m which corresponds to the drain spacing of 2.4 m of the square wick drains mesh under area 2. Table 13 synthesizes all the calculated D_{eq} values.

It was then decided to use the following procedure to theoretically predict the course of compression of layer 6 under area 1 and under area 2:

• the course of the primary compression was calculated using Barron (1948) formulation considering the “pseudo final primary compression” (ΔH_p)’ calculated as already mentioned, under the “pseudo final effective stresses”,

• the course of the secondary compression was calculated using the formulas of Carvalho, isolating the secondary compression from primary compression, considering it to occur in a layer drained vertically with a drainage distance equal to D_{eq} with the “pseudo final secondary compression” value (ΔH_s)’ and,

• sum the two above compressions to get the course of the total compression.

It was decided to call this method: “Primary Barron + secondary pseudo Taylor and Merchant”.

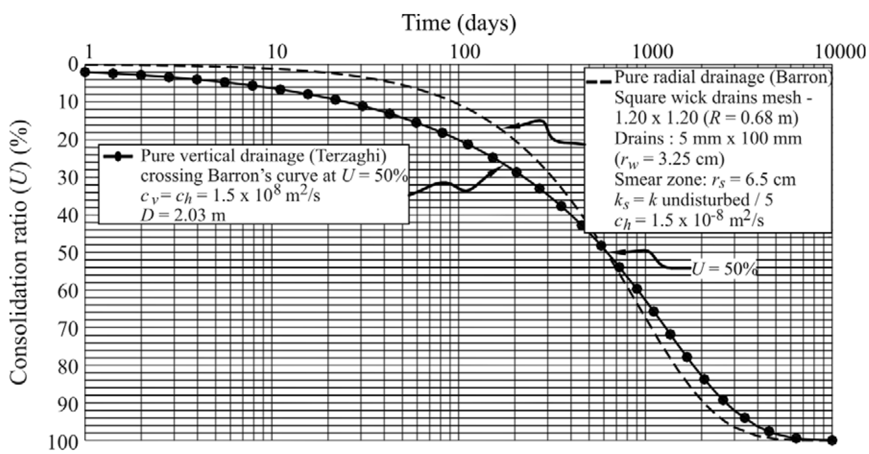

Figure 30 - Comparison of primary consolidation ratio between a clay layer with pure vertical drainage with $c_v = 1.5 \times 10^{-8}$ m^2/s and a clay layer with a 1.2 m x 1.2 m square mesh of wick drains (pure radial drainage) with $c_h = c_v = 1.5 \times 10^{-8}$ m^2/s .

Table 13 - D_{eq} values.

Area	c_h/c_v (*)	r_s	D_{eq}	Area	c_h/c_v (*)	r_s	D_{eq}
	1	6.5 cm	2.03 m		1	6.5 cm	4.33 m
1	3	6.5 cm	1.16 m	2	3	6.5 cm	2.49 m
	1	19.5 cm	2.67 m		1	19.5 cm	5.89 m

(*) ratio of c_h of layer 6 to the assumed value of c_v of the equivalent layer with vertical drainage.

13.2. Backanalysis of layer 6 compression under area 1

Under area 1, the "pseudo final effective stress" at mid-height of layer 6, "σ_v - u_{hid}" is equal to 221.3 kPa compared to σ'_{vi} = 81.2 kPa and σ'_p (lab) = 187.1 kPa and is, in fact, higher than the (real) final effective stress, equal to 201.6 kPa, to be reached after full primary and full secondary consolidations when the total settlement will be 4.20 m whereas the total settlement at the end of october 2009 was 2.36 m.

The primary and secondary compressions were then calculated considering that this "pseudo final effective stress" would be maintained constant thereafter, obtaining:

• "pseudo final primary compression" (ΔH_p)': 68 cm which is, in fact, higher than the (real) final primary compression to be reached after full primary consolidation which is equal to 43 cm as indicated in Table 6.

• "pseudo final secondary compression" (ΔH_s)': 177 cm which is, in fact, equal to the (real) final secondary compression to be reached after full secondary consolidation as indicated in Table 6 and their sum:

• the "pseudo final total compression" (ΔH_t)': 245 cm which is, in fact, higher than the (real) final total compression to be reached after full primary and full secondary consolidations which is equal to 220 cm.

It was immediately found out that no satisfying adjustment was to be obtained with only one constant value of c_h over the whole period. Figure 31 shows the theoretical curve obtained following the above described "Primary Barron + secondary pseudo Taylor and Merchant" procedure reasonably well fitted to the measured compression curve of layer 6 under the center of area 1 for the value of c_h of layer 6 equal to the value of c_v of the equivalent layer with vertical drainage and r_s = 6.5 cm.

This adjustment was achieved by dividing the total measurement period into two periods. As can be seen on Fig. 31, the values of c_h which led to the adjustment of the theoretical curve to the measured one are:

• for the first period: $c_h = 5 \times 10^{-8}$ m^2/s,

• for the second period: $c_h = 2.3 \times 10^{-8}$ m^2/s.

It has to be pointed out that in the above analysis, the vertical drainage in layer 6 has not been taken into account for considering that it would not affect significantly the results of the back-analysis.

Table 14 summarizes the results of the back-analysis of layer 6 compression with vertical drainage under the center of area 1 through the "Primary Barron + secondary pseudo Taylor and Merchant" procedure indicating:

• the equivalent time at the end of each period,

• the coefficient of consolidation for which the best fit was obtained between the theoretical curve and the measured compression curve, in each period: c_h during period 1, c_h during period 2,

• the total compression ΔH_{tj} measured at the end of each period,

• the calculated primary compression, ΔH_{pj} and secondary compression, ΔH_{sj} at the end of period 1 and period 2,

• the calculated ratio of the primary compression at the end of each period ΔH_{pj} to the "pseudo final primary compression" (ΔH_p)' called the "primary consolidation index",

• the calculated ratio of the secondary compression at the end of each period ΔH_{sj} to the "pseudo final secondary

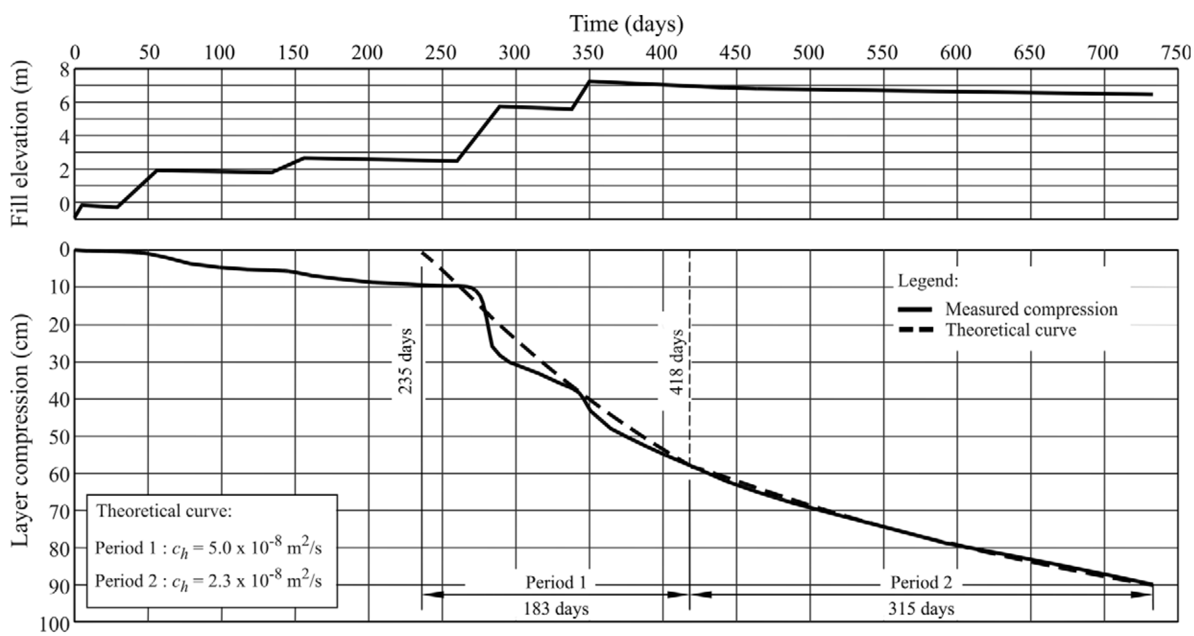

Figure 31 - Theoretical curve reasonably well fitted to the measured compression curve of layer 6 under the center of area 1.

compression" (ΔH_s)' called the "secondary consolidation index",

• the calculated ratio of the total compression at the end of each period ΔH_{tj} to the "pseudo final total compression" (ΔH_t)' called the "aggregate consolidation index".

Repeating the adjustment of a theoretical curve to the measured compression curve for the value of c_h of layer 6 equal to three times the value of c_v of the equivalent layer with vertical drainage and r_s = 6.5 cm, and for r_s = 19.5 cm, for the same two periods as above, the same good adjustments were obtained for the values of c_h shown in Table 15, with all other values identical to the ones shown in Table 14.

An can be seen the ratio of the c_h value in layer 6 to the c_v value admitted to determine the drainage distance of the equivalent layer with vertical drainage has no effect on the backanalyzed value of c_h.

As already mentioned in the backanalysis of layer 6 under area 3, it can be assumed that the value of the average primary consolidation ratio $\overline{U}_p$ is equal to the primary consolidation index $[\Delta H_{pj}/(\Delta H_p)']$, so that the average vertical effective stress in layer 6 at the end of each period can be computed from the following formula:

$$\sigma'_v = \sigma'_{vi} + [(\sigma_v - u_{hid}) - \sigma'_{vi}] \text{ x } \overline{U}_p = \sigma'_{vi} + [(\sigma_v - u_{hid}) - \sigma'_{vi}] \text{ x } [\Delta H_{pj}/(\Delta H_p)'] \quad (9)$$

allowing then, to plot the back-analyzed values of c_h against the mean effective vertical stress σ'_v in layer 6 in area 1, as shown in Fig. 32.

It can be seen in Fig. 32 that the obtained results are in good agreement with the observation that it has to be expected that the vertical effective stress at which the coefficient of consolidation field value passes from its higher value in the recompression range, to its lower value in the virgin compression range, is to be smaller than the σ'_p value determined in the oedometer tests. It can also be observed that the back-analyzed c_h field values are also in good agreement with the c_v laboratory values in the transition range between the recompression range and the virgin compression range.

13.3. Backanalysis of layer 6 compression under area 2

In area 2, the last phase of heightening the fill was postponed due to lack of fill material. For this reason, one set of values of "pseudo final effective stress", "pseudo final primary compression" and "pseudo final secondary compression" had to be used for t up to 450 days and another set of values had to be used for t > 450 days.

Under area 2, the "pseudo final effective stress" at mid-height of layer 6, "$\sigma_v - u_{hid}$" is equal to 205.9 kPa up to t = 450 days and equal to 221.9 kPa for t > 450 days, compared to σ'_{vi} = 86.6 kPa and σ'_p (lab) = 192.5 kPa and is, in fact, higher than the (real) final effective stress, equal to 198.3 kPa, to be reached after full primary and full secondary consolidations when the total settlement will be 3.89 m whereas the total settlement at the end of october 2009 was 1.46 m.

The primary and secondary compressions were then calculated considering that this "pseudo final effective stress" would be maintained constant thereafter, obtaining:

Table 15 - Values of c_h yielded by the back analysis.

c_h/c_v (*)	r_s	D_{eq}	c_h for Period 1	c_h for Period 2
1	6.5 cm	2.03 m	5.0×10^{-8} m^2/s	2.3×10^{-8} m^2/s
3	6.5 cm	1.16 m	5.0×10^{-8} m^2/s	2.3×10^{-8} m^2/s
1	19.5 cm	2.67 m	8.6×10^{-8} m^2/s	4.2×10^{-8} m^2/s

(*) ratio of c_h of layer 6 to the assumed value of c_v of the equivalent layer with vertical drainage.

Table 14 - Results of the back analysis of layer 6 compression under the center of area 1 for the value of c_h of layer 6 equal to the value of c_v of the equivalent layer with vertical drainage and r_s = 6.5 cm.

	Period 1	Period 2
Time t (equivalent) at the end of each period	183 days	498 days
Back analyzed c_h value for each period	5.0×10^{-8} m^2/s	2.3×10^{-8} m^2/s
ΔH_{tj}: Total compression of layer 6 measured at the end of each period	58 cm	90 cm
ΔH_{pj} compression at the end of each period obtained from "Primary Barron + secondary pseudo Taylor and Merchant" calculations	34 cm	49 cm
$\Delta H_{pj}/(\Delta H_p)$' Primary consolidation index at the end of each period	34/68 = 50%	49/68 = 72%
ΔH_{sj} compression at the end of each period obtained from "Primary Barron + secondary pseudo Taylor and Merchant" calculations	24 cm	41 cm
$\Delta H_{sj}/(\Delta H_s)$' Secondary consolidation index at the end of each period	24/177 = 14%	41/177 = 23%
$\Delta H_{tj}/(\Delta H_t)$' Total consolidation index at the end of each period	58/245 = 24%	90/245 = 37%

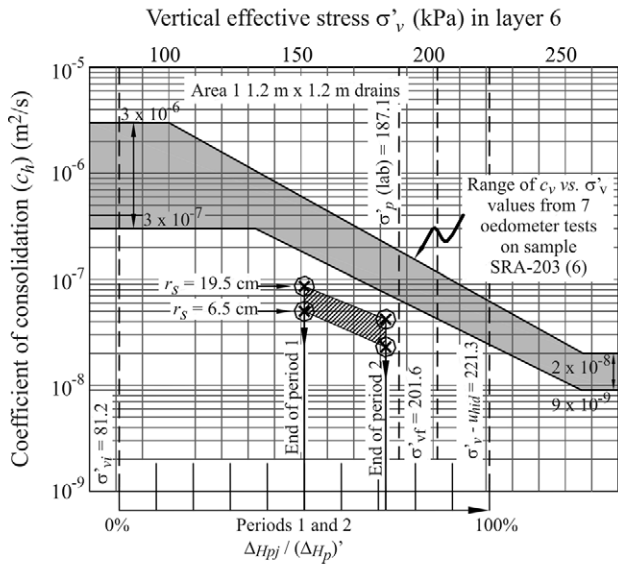

Figure 32 - Back-analyzed values of c_h *vs.* mean effective vertical stress in layer 6 under area 1.

• "pseudo final primary compression" (ΔH_p)': 34 cm for t up to 450 days and 51 cm for t > 450 days for which is, in fact, higher than the (real) final primary compression to be reached after full primary consolidation which is equal to 26 cm as indicated in Table 7.

• "pseudo final secondary compression" (ΔH_s)': 153 cm for t up to 450 days and 153 cm for t > 450 days which is, in fact, equal to the (real) final secondary compression to be reached after full secondary consolidation as indicated in Table 7 and their sum:

• the "pseudo final total compression" (ΔH_t)': 187 cm for t up to 450 days and 204 cm for t > 450 days which is, in fact, higher than the (real) final total compression to be reached after full primary and full secondary consolidations which is equal to 179 cm.

It was immediately found out that no satisfying adjustment was to be obtained with a constant value of c_h (and c_v) over the whole period. Figure 33 shows the theoretical curve obtained following the above described "Primary Barron + secondary pseudo Taylor and Merchant" procedure reasonably well fitted to the measured compression curve of layer 6 under the center of area 2 for the value of c_h of layer 6 equal to the value of c_v of the equivalent layer with vertical drainage and r_s = 6.5 cm.

This adjustment was achieved by dividing the total measurement period into three periods with period 1 up to t = 450 days and periods 2 and 3 for t > 450 days. As can be seen on Fig. 33, the values of c_h which led to the adjustment of the theoretical curve to the measured one are:

• for the first period: c_h = 9 x 10^{-8} m^2/s,

• for the second period: c_h = 9 x 10^{-8} m^2/s,

• for the third period: c_h = 4.5 x 10^{-8} m^2/s.

Table 16 summarizes the results of the back-analysis of layer 6 compression with vertical drainage under the center of area 2 through the "Primary Barron + secondary pseudo Taylor and Merchant" procedure indicating:

• the equivalent time at the end of each period,

• the coefficient of consolidation for which the best fit was obtained between the theoretical curve and the measured compression curve, in each period: c_h during period 1, c_h during period 2, c_h during period 3,

• the total compression ΔH_{tj} measured at the end of each period,

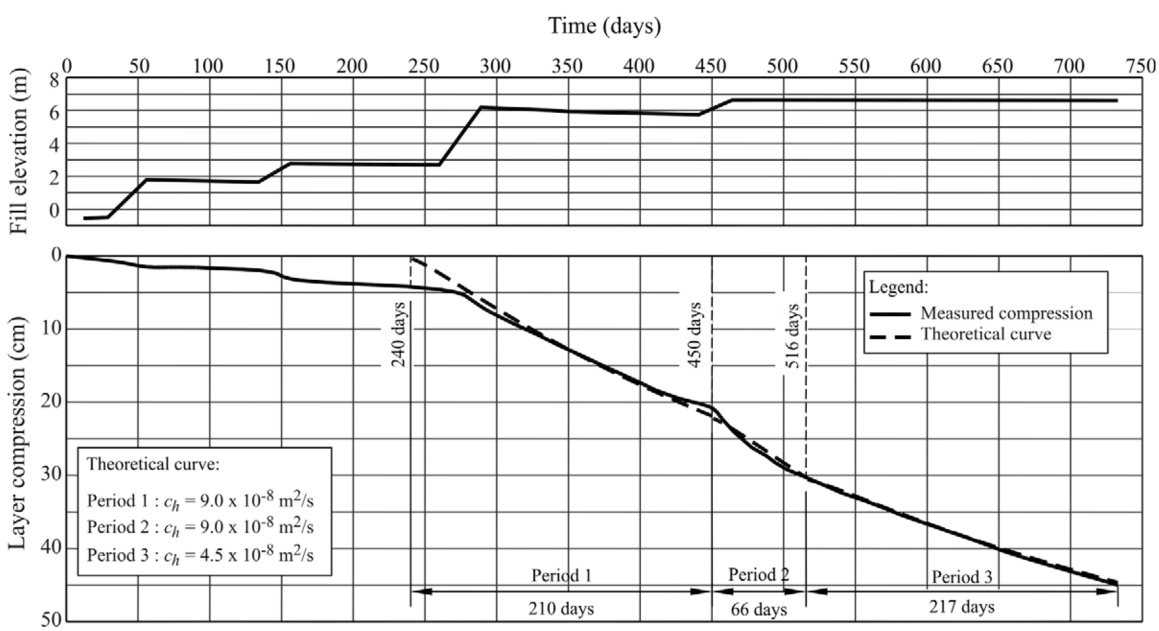

Figure 33 - Theoretical curve reasonably well fitted to the measured compression curve of layer 6 under the center of area 2.

• the calculated primary compression, ΔH_{pj} and secondary compression, ΔH_{sj} at the end of period 1, period 2 and period 3,

• the calculated ratio of the primary compression at the end of each period ΔH_{pj} to the "pseudo final primary compression" (ΔH_p)' called the "primary consolidation index",

• the calculated ratio of the secondary compression at the end of each period ΔH_{sj} to the "pseudo final secondary compression" (ΔH_s)' called the "secondary consolidation index",

• the calculated ratio of the total compression at the end of each period ΔH_{tj} to the "pseudo final total compression" (ΔH_t)' called the "aggregate consolidation index".

Repeating the adjustment of a theoretical curve to the measured compression curve for $c_h = 3\ c_v$ and for r_s = 19.5 cm, for the same three periods as above, the same good adjustments were obtained for the values of c_h shown in Table 17, with all other values identical to the ones shown in Table 16.

As already mentioned in the backanalysis of layer 6 under areas 3 and 1, the back-analyzed values of c_h can be plotted against the mean effective vertical stress σ'_v in layer 6 as shown in Fig. 34.

It can be seen in Fig. 34 that the obtained results are in good agreement with the observation that it has to be expected that the vertical effective stress at which the coefficient of consolidation field value passes from its higher value in the recompression range, to its lower value in the virgin compression range, is to be smaller than the σ'_p value determined in the oedometer tests. It can also be observed that the back-analyzed c_h field values are also in good

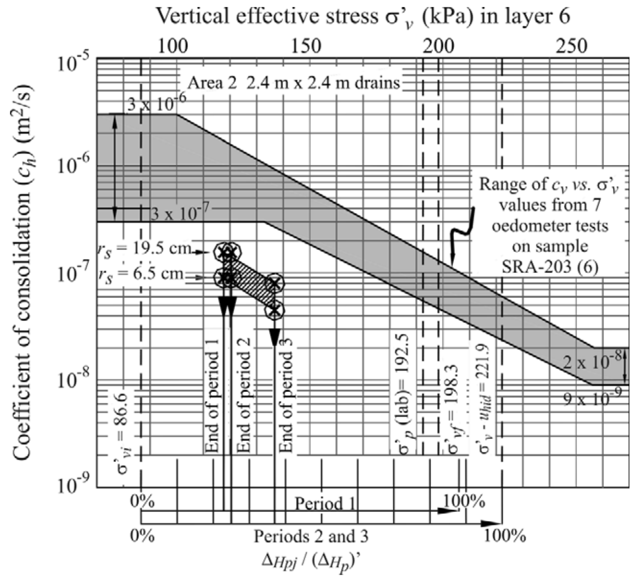

Figure 34 - Back-analyzed values of c_h *vs.* mean effective vertical stress in layer 6 under area 2.

Table 16 - Results of the back analysis of layer 6 compression under the center of area 2 for the value of c_h of layer 6 equal to the value of c_v of the equivalent layer with vertical drainage and r_s = 6.5 cm.

	Period 1	Period 2	Period 3
Time *t* (equivalent) at the end of each period	210 days	276 days	493 days
Back analyzed c_h value for each period	9.0 x 10^{-8} m²/s	9.0 x 10^{-8} m²/s	4.5 x 10^{-8} m²/s
ΔH_{tj}: Total compression of layer 6 measured at the end of each period	22 cm	30 cm	45 cm
ΔH_{pj} compression at the end of each period obtained from "Primary Barron + secondary pseudo Taylor and Merchant" calculations	9 cm	13 cm	19 cm
$\Delta H_{pj}/(\Delta H_p)$' Primary consolidation index at the end of each period	9/34 = 26%	13/51 = 25%	19/51 = 37%
ΔH_{sj} compression at the end of each period obtained from "Primary Barron + secondary pseudo Taylor and Merchant" calculations	13 cm	17 cm	26 cm
$\Delta H_{sj}/(\Delta H_s)$' Secondary consolidation index at the end of each period	13/153 = 9%	17/153 = 11%	26/153 = 17%
$\Delta H_{tj}/(\Delta H_t)$' Total consolidation index at the end of each period	22/187 = 12%	30/204 = 15%	45/204 = 22%

Table 17 - Values of c_h yielded by the back analysis.

c_h/c_v	r_s	D_{eq}	c_h for Period 1	c_h for Period 2	c_h for Period 3
1	6.5 cm	4.33 m	9.0 x 10^{-8} m²/s	9.0 x 10^{-8} m²/s	4.5 x 10^{-8} m²/s
3	6.5 cm	2.49 m	9.0 x 10^{-8} m²/s	9.0 x 10^{-8} m²/s	4.5 x 10^{-8} m²/s
1	19.5 cm	5.69 m	15.5 x 10^{-8} m²/s	15.5 x 10^{-8} m²/s	8.0 x 10^{-8} m²/s

(*) ratio of c_h of layer 6 to the assumed value of c_v of the equivalent layer with vertical drainage.

agreement with the laboratory c_v values in the transition range between the recompression range and the virgin compression range.

It has to be pointed out that in the above analysis, the vertical drainage in layer 6 has not been taken into account, although in the case of area 2, the Deq value is of the same order of magnitude as the vertical drainage distance equal to 4.75 m, as shown in Table 13. Taking the contribution of the vertical drainage into account would certainly have some influence on the obtained results and would, lead in this case to somewhat smaller values of c_h.

14. Comments on the Current Method Used to Analyze Embankments Settlements

As mentioned in item 9, the current method used to back-analyze embankments settlements is Asaoka's method which, as already discussed, is applied considering that the secondary settlement only starts occurring after the end of the primary settlement.

Now what happens when Asaoka's method is applied to a compression curve which reflects the simultaneous occurrence of primary and secondary compressions as modeled by a Taylor and Merchant curve?

Figure 35 shows a theoretical Taylor and Merchant's curve where 50% of the total compression is due to primary consolidation and the other 50% is due to secondary consolidation (r = 0.5). All input parameters are shown in Fig. 35.

The plain dotted line represents the known part of the total compression (primary + secondary) curve which is the one that is known from settlement monitoring up to t = 220 days. It is this part of the curve, between t = 40 days and t = 220 days after the end of construction, to which Asaoka's method is commonly applied, considering that:

- the secondary consolidation has not started yet and
- the primary consolidation ratio is higher than 33% (Massad, 2009), since, according to Massad: "The formula $U = 1\text{-}0.811\ e^{ct}$ where $c = 2.5\ c_v/(H_d)^2$ yields the value of the vertical consolidation ratio of Terzaghi's theory for $U \geq 60\%$ (Taylor, 1948)" and "Asaoka's method applicable range can be extended to $U \geq 33\%$ through the use of another exponential function which gives the value of the consolidation ratio in function of the time factor (Schofield & Wroth 1968, p. 79)."

Figure 36 shows Asaoka's construction applied to the measured values of the "supposed" primary compression varying from 12 cm at t = 40 days to 18 cm at t = 220 days.

As can be seen, the total primary compression thus obtained is 44 cm. From this value the primary consolidation ratio which is obtained at the end of the period is 1 8 cm: 44 cm = 41%.

Moreover, the c_v value obtained from Asaoka's construction equal to 5.7 x 10^{-7} m^2/s is 57 times higher than the real c_v value equal to 1.0 x 10^{-8} m^2/s.

At this point, most Asaoka's method users observe that all compression values higher than 14.5 cm satisfy the condition U > 33% which is then invoked to vouch for the validity of the results thus obtained.

Figure 37 compares the real compression curves (as represented by input Taylor and Merchant primary and total compression curves) with the predicted primary compression curve obtained using Asaoka's method and the predicted total compression curve predicted through Asaoka's method + $C\alpha$ (secondary). The Asaoka (primary) + $C\alpha$

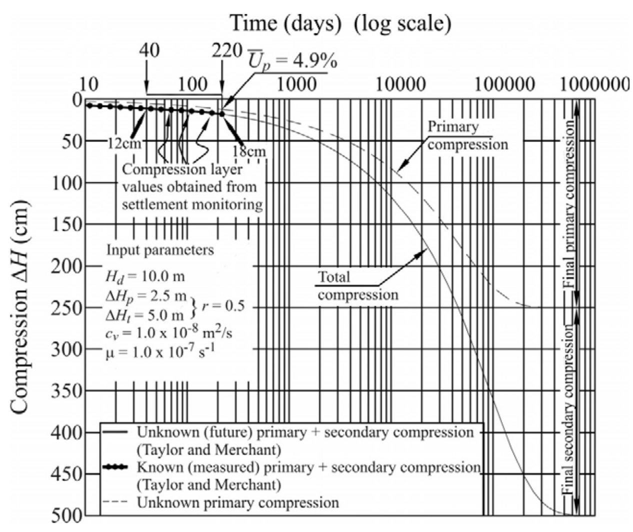

Figure 35 - Taylor and Merchant theoretical curve for r = 0.5.

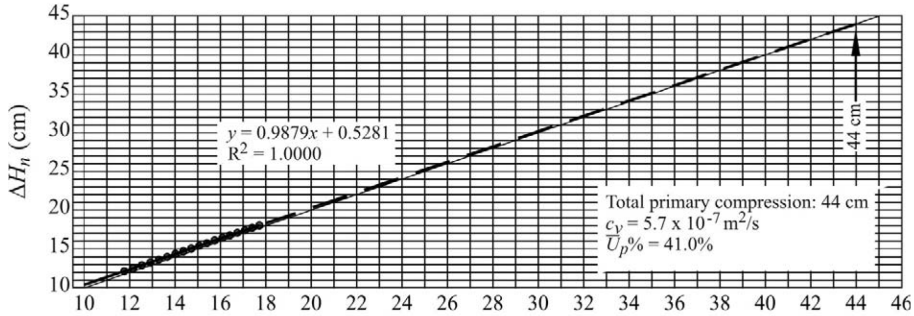

Figure 36 - Asaoka's construction applied to the part of the dotted curve of Fig. 35 between t = 40 days and t = 220 days.

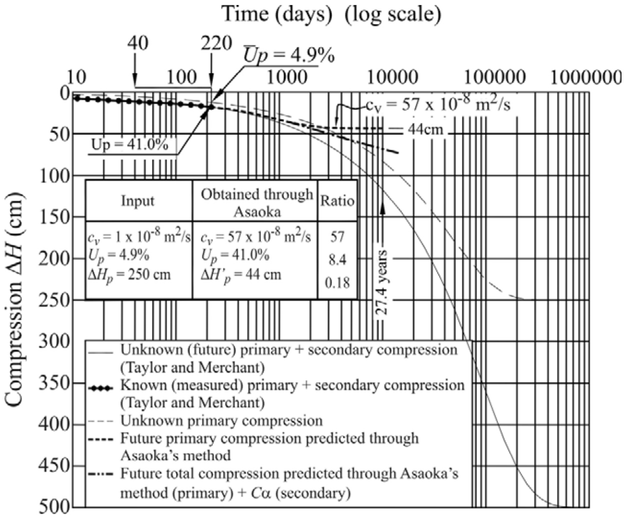

Figure 37 - Comparison of the real compression curves (as represented by input Taylor and Merchant primary and total compression curves) with the predicted primary compression curve obtained using Asaoka's method and the predicted total compression curve predicted through Asaoka's method + $C\alpha$ (secondary).

(secondary) curve illustrates the type of total compression curve which would be commonly considered in the design by drawing a straight line based on the laboratory value of $C\alpha$ tangent to the primary compression obtained through Asaoka's method.

As can be seen, the results obtained through Asaoka's method in this situation, a rather realistic situation in the authors' eyes, are totally mistaken, leading to overestimate by a factor of 57 the value of c_v. At the same time the final primary settlement is grossly underestimated as being only 18% of the real final primary settlement and the consolidation ratio at the end of the reading period is grossly overestimated, *i.e.* 41.0% against 4.9%.

Table 18 shows the results of Asaoka's method applied during the period from 40 to 220 days using $\Delta t = 10$ days to a number of known layer compression (primary plus secondary) *vs.* time curves of the Taylor and Merchant's type including the case presented above.

As can be seen in Table 18, the degree of discrepancy between the real values and the back analyzed values varies widely depending on the importance of the secondary compression (r value), the thickness of the layer (H_d) and the value of the coefficient of consolidation (c_v).

All back analyzed values, that is total primary settlement, consolidation ratio at the end of the monitoring period and c_v values, may be grossly underestimated in some cases and grossly overestimated in others. And it can be noted that the largest discrepancies concern the c_v value

Table 18 - Results of Asaoka's method applied to known layer compression (primary + secondary) *vs.* time curves of the Taylor and Merchant's type(*).

Input values							Back analyzed values through Asaoka's method			Ratio of back analyzed values over input values		
r	H_d (m)	ΔH_t (m)	ΔH_p (m)	C_v (m²/s)	ΔH^* (cm)	U_p^* (%)	$\Delta H'_p$ (m)	$U_p^{*\prime}$ (%)	C'_v (m²/s)	$\frac{\Delta H'_p}{\Delta H'_p}$	$\frac{U_p^{*\prime}}{U_p^*}$	$\frac{c'_v}{c_v}$
0.2	1.0	0.50	0.10	2 x 10⁻⁷	34.7	100	0.48	72	2.5 x 10⁻⁸	4.80	0.72	0.1
	4.0	2.00	0.40	2 x 10⁻⁷	43.2	55	0.85	51	2.1 x 10⁻⁷	2.13	0.92	1.1
	10.0	5.00	1.00	2 x 10⁻⁷	44.1	22	0.94	47	1.1 x 10⁻⁶	0.94	2.13	5.5
0.5	1.0	0.50	0.25	1 x 10⁻⁸	16.0	49	0.28	57	1.6 x 10⁻⁸	1.12	1.16	1.6
	1.0	0.50	0.25	5 x 10⁻⁸	33.0	92	0.45	73	2.5 x 10⁻⁸	1.80	0.80	0.5
	4.0	2.00	1.00	1 x 10⁻⁸	15.9	12	0.29	55	2.2 x 10⁻⁷	0.29	4.56	22
	4.0	2.00	1.00	5 x 10⁻⁸	35.9	28	0.62	58	2.5 x 10⁻⁷	0.62	2.11	5.0
	10.0	5.00	2.50	1 x 10⁻⁸	18.0	4.9	0.44	41	5.7 x 10⁻⁷	0.18	8.33	57
	10.0	5.00	2.50	5 x 10⁻⁸	36.3	11	0.67	54	1.3 x 10⁻⁶	0.27	4.93	26
0.8	1.0	0.50	0.40	1 x 10⁻⁸	21.3	49.2	0.32	67	2.0 x 10⁻⁸	0.80	1.35	2.0
	4.0	2.00	1.60	1 x 10⁻⁸	21.4	12.3	0.33	65	3.0 x 10⁻⁷	0.21	5.27	30
	10.0	5.00	4.00	1 x 10⁻⁸	29.8	6.9	0.47	64	8.5 x 10⁻⁷	0.12	9.23	85

(*) r = ratio of the primary settlement over the total settlement, H_d = drainage distance (= half the layer thickness), ΔH_t = layer total final compression, ΔH_p = layer primary final compression, c_v = vertical coefficient of consolidation, ΔH^* = layer total compression at t = 220 days, U_p^* = primary consolidation ratio at t = 220 days, $\Delta H'_p$ = layer primary final compression obtained through Asaoka's method, $U_p^{*\prime}$ = primary consolidation ratio at t = 220 days obtained through Asaoka's method, c'_v = vertical coefficient of consolidation obtained through Asaoka's method.

which varies from being underestimated by a factor of 10 to being overestimated by a factor of 85.

All these discrepancies are provoked by, and only by, the facts that the settlements occurring due to secondary compression are wrongly taken as part of the primary compression by Asaoka's method and that analyzed settlement values correspond to ratio consolidation values outside the proper range for which the method was devised.

As already mentioned, "when secondary compression and primary compression occur simultaneously, the volume of water expelled is larger than the volume of water which would be expelled if only primary consolidation took place. Since the initial pore pressure and gradient are not affected by the phenomenon of secondary consolidation, then the pore pressure dissipation has to be slower when secondary consolidation occurs simultaneously with primary consolidation than if it did not", which means that in this case the course of pore pressure dissipation departs from Terzaghi's theory and that the Asaoka procedure applied to the pore pressure measurements as proposed by Orleach (1983) might also lead to erroneous results.

15. Conclusions

The results obtained from the back-analysis of the SFL layer compression under area 3, with vertical drainage, performed making use of Taylor and Merchant's theory as presented in item 12 and of the results obtained from the back-analysis of the SFL layer compressions under areas 1 and 2, with radial drainage, making use of the so called "Primary Barron + secondary pseudo Taylor and Merchant" procedure as presented in item 13 in conjunction with the results of the good quality laboratory oedometer tests are synthesized in Fig. 38.

These results are presented in terms of coefficient of consolidation, in log scale, plotted *vs.* the mean vertical effective stress in the soft clay layer, in natural scale, relative to preconsolidation stresses values.

The darker shaded zone delimits the range of all c_v values determined from 7 standard oedometer tests run on an excellent quality undisturbed sample extracted close to the middle of the soft clay layer. The lighter grey hatched vertical zones indicate the range of preconsolidation stress (σ'_p) values obtained in the oedometer tests and the ranges of initial vertical effective stresses (σ'_{vi}) and of preconsolidation stresses (σ'_p) at mid height of the soft clay layer under the three embankment areas.

The observation of Fig. 38 leads to some very interesting conclusions which are presented hereafter.

• Conclusions regarding the variation of the value of c_v measured in the laboratory oedometer test with the effective stress

It can be seen in Fig. 38 that the c_v value measured in the laboratory is constant for σ'_v values up to σ'_p - 80 kPa, then decreases by a factor of almost 100 when σ'_v increases from σ'_p - 80 kPa up to σ'_p + 80 kPa, and is then constant for σ'_v values higher than σ'_p + 80 kPa up to the maximum stress presented in the graph.

As shown on Fig. 4 the c_v value for the totally remolded sample is much smaller than the c_v value for the undisturbed sample for effective stresses up to σ'_p + 80 kPa, but it

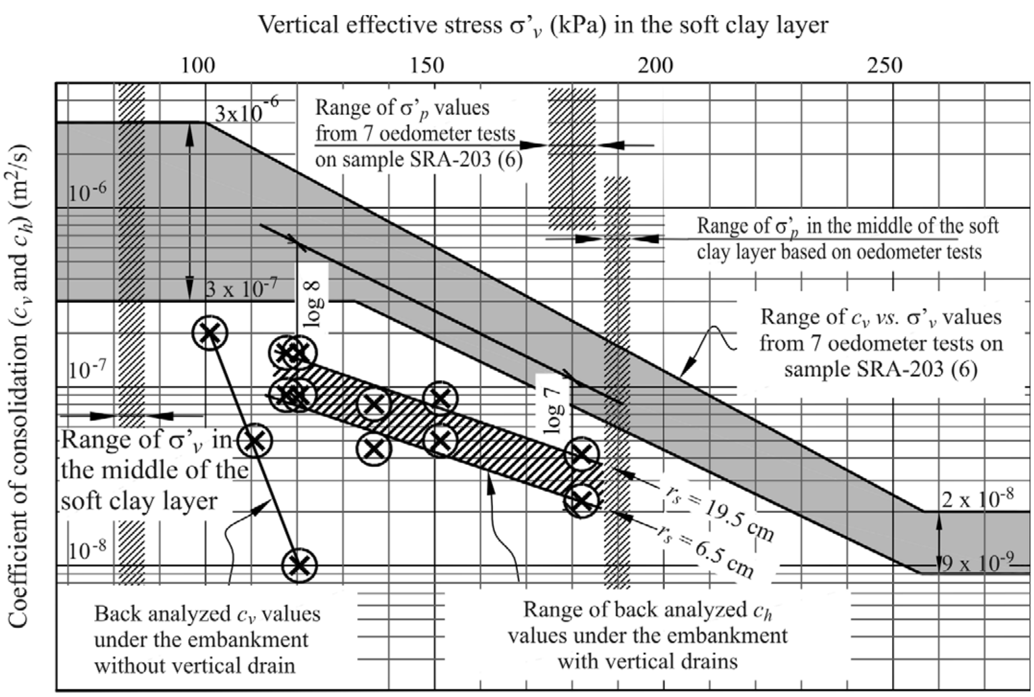

Figure 38 - Back analyzed values of field c_v and c_h *vs.* mean effective vertical stress in the soft clay layer.

is equal to the c_v value of the undisturbed clay for effective stress values above σ'_p + 80 kPa.

• Conclusions regarding the coefficient of consolidation values, c_v and c_h in the field obtained through the back-analysis of the SFL clay layer measured compressions

1. It is rather remarkable that the c_h values obtained from two totally distinct compression curve segments of layer 6, for period 1 and period 2 under area 2 for about the same value of σ'_v, are identical.

The two lines which delimit the hatched range of back analyzed c_h values under the embankment with vertical drains, that is with radial drainage, defined by ten points, show the tendency of the values of c_h to decrease when the applied effective stress increases. This decrease is very similar to the decrease of the c_v value measured in the oedometer test. This decrease is very significant even for values of σ'_v much smaller than the laboratory preconsolidation stress σ'_p and the decrease of the c_h value in the field takes place for smaller values of σ'_v than the decrease of c_v in the laboratory as should be expected, as already mentioned, due to the fact that the apparent consolidation stress (or the "yielding stress") decreases when the strain rate (which is much smaller in the field than in the laboratory) decreases.

2. In the case of vertical drainage, the values of c_v measured in the field under area 3 with no wick drain decrease much more sharply than in the case of radial drainage as shown by the plain line which goes through the points of the back analyzed c_v values under the embankment without vertical drain. The very fast decrease of the c_v value under area 3 is attributed to the fact that close to the top and to the bottom of the clay layer, the local consolidation ratio reaches values above 80% right at the beginning of the consolidation, with σ'_v close to the "pseudo final effective stress" "σ_v - u_{hid}" and since at this stress level the c_v value is close to the small virgin compression range value, then the top and bottom sublayers have a "sealing" effect on the vertical drainage of the sublayers in the middle of layer 6.

Figure 39 shows the primary consolidation ratio profile with depth within layer 6 under area 3 with no wick drain for the situation at the end of period 3 when the average primary consolidation ratio in the layer is equal to 40% as indicated in Table 12.

Of course, in the two areas with vertical drains the same high consolidation ratio and small c_v value also exist close to the top and to the bottom of the layer, but since the radial drainage is the predominant one, in this case these "sealing sublayers" have little effect on the consolidation of the layer.

3. For a given value of vertical effective stress, the value of c_v and of c_h measured in the field is quite smaller than the value of c_v measured in the laboratory oedometer test at least within the backanalyzed range and rather probably up to σ'_p + 80 kPa. In fact for the SFL Santos clay, it can be seen that the back analyzed c_h values under the embankment with vertical drains within the stress range shown in Fig. 38 are somewhere around 7 to 8 times smaller than the values of c_v in the oedometer tests up to σ'_p, with this difference decreasing as σ'_v increases. This is believed to be partly due to the already mentioned fact that the apparent "yielding stress" is smaller in the field than in the laboratory and partly due to the effect of the smeared zone around the drains.

• Conclusions regarding the efficiency of preloading with wick drains

If, as advocated by various authors like Saye (2001) the driving of the wick drains had the effect of remoulding a large volume of soil around the drains up to the point of remoulding the whole soft clay volume in the case of closely spaced drains as is the case under area 1, then the back-analyzed c_h values would not behave as shown in Fig. 37, in fact c_h values under area 1 would be much

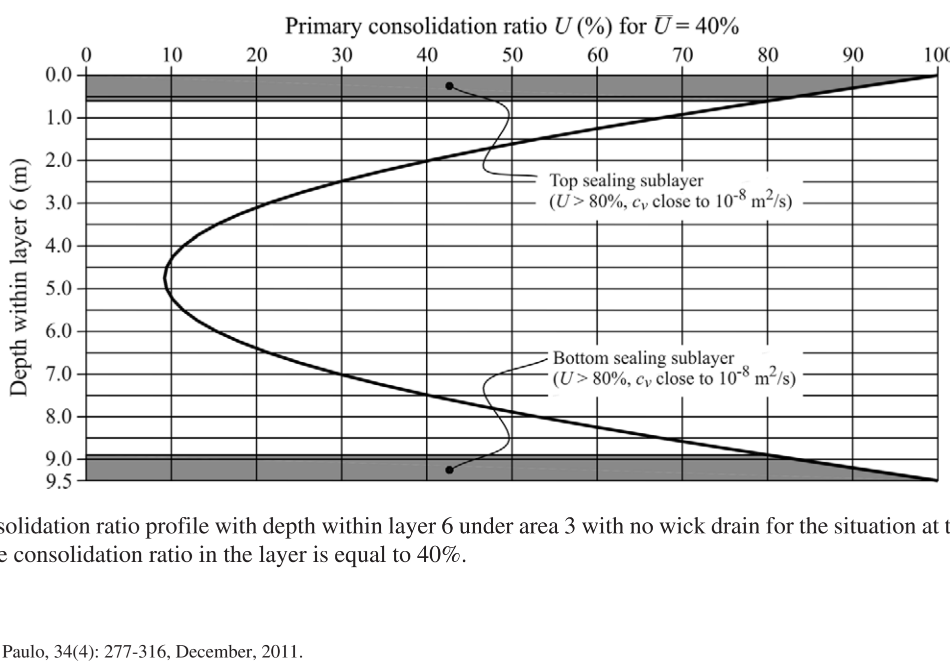

Figure 39 - Consolidation ratio profile with depth within layer 6 under area 3 with no wick drain for the situation at the end of period 3 when the average consolidation ratio in the layer is equal to 40%.

smaller than the c_h values under area 2 even for lower consolidation ratios. This is, obviously, not the case and since the coefficient of consolidation of the soil mass between the 1.2 m spaced drains is identical to the coefficient of consolidation of the soil mass between the 2.4 m spaced drains, then it can be concluded that the 1.2 m spaced drains are totally efficient in reducing the time for the primary settlement to occur by the factor of 4 ($2.4^2/1.2^2$) which is really expected from them showing, thus, their perfect efficacy. As can be clearly observed in Figs. 32, 34 and 38, this holds true whether the smeared zone radius is only 6.5 cm or 19.5 cm for the permeability ratio ks/k = 1/5. It has to be mentioned that this permeability ratio must come close to 1 for $\sigma'_v > \sigma'_p$ + 80 kPa since c_v of the remolded soil comes close to c_v of the undisturbed soil in this stress range.

This result, which is contrary to many alleged published statements based on disputable results obtained through back-analysis not taking into account the simultaneous occurrence of secondary and primary consolidations, corroborates the asian and european practice where 1 meter spaced drains are most commonly used and where even smaller spacings are also used as in the case of the 0.5 m and 0.6 m spacings used in the Airbus A-380 factory site in Hamburg (Varaksin 2010).

• Conclusions regarding the working hypothesis

As mentioned in item 9, the conclusion that the c_v value measured in the field is discrepant from the c_v value measured in the laboratory, with the c_v field value typically 10 to 100 times higher than the c_v lab value, which has been repeatedly reached based on the working hypothesis that secondary consolidation would only start after the end of primary consolidation, needs, for its justification, to invoke the presence of providential very thin, continuous, layers of pervious sand, which is considered by the authors to be very far-fetched.

In many cases, this discrepancy might be due to the fact that the c_v value of the field conditions has been obtained for stress levels within the recompression or transition range since the $\Delta\sigma_v$ applied by field embankments to the foundations are normally quite small whereas the c_v value of the lab conditions has been taken as the value which corresponds to higher stress levels, within the virgin compression range, since no mention is made in most published papers about the stress levels at which these c_v values were determined.

As mentioned in item 14, in the cases when c_v values in the field and in the laboratory are compared for the same stress level, this discrepancy is provoked by, and only by, the facts that the settlements occurring due to secondary compression have been wrongly taken as part of the primary compression by Asaoka's method and all other methods based on the working hypothesis that secondary consolidation only starts after the end of primary consolidation and that analyzed settlement values correspond to ratio consolidation values outside the proper range for which the method was devised.

The conclusions reached by the authors regarding the coefficient of consolidation values c_v and c_h in the field obtained through the back-analysis of the SFL clay layer measured compressions are, on the contrary, in perfect agreement with what should be expected from common sense and from soil mechanics basic understanding of soil behavior.

This leads the authors to conclude that the working hypothesis which consists in considering that, in the field, primary consolidation and secondary consolidation occur simultaneously is the only realistic hypothesis which should be adopted. This conclusion has also been reached by most soil mechanics institutes around the world and is quickly being incorporated in engineering standards mainly in european countries.

• Conclusions regarding the high quality standard and special oedometer tests

As shown in item 3 the high quality standard oedometer tests provided reliable values of the compressibility parameters C_c and C_r and of the preconsolidation stress σ'_p which are critically important for the final design and construction of the terminal but which were not reliably known at the end of the basic design due to typical "highly scattered lab data resulting from poor quality samples" as pointed out by Ladd (2008). As shown in item 5, the high quality special oedometer tests provided the OCR value equivalent to the end of secondary consolidation, a value which is not normally called for by the designers who take for granted that secondary consolidation never finishes. The preconsolidation stresses measured in the high quality oedometer tests are much higher than the ones obtained from the large quantity of tests run during the basic design. Furthermore their values agree quite well with the OCR value equivalent to the end of secondary consolidation, defined as being equal to 2.1 in item 5, since the lab results show σ'_p values higher than 2.1 σ'_v above 15.5 m and close to 2.1 σ'_v below 15.5 m within the SFL layer. This agreement validates theses values. As has to be expected, the C_c values of the high quality oedometer tests are also quite higher than the ones obtained from the large quantity of tests run during the basic design. It also has to be mentioned that both the C_c and σ'_p values obtained from the high quality tests are quite higher than the C_c and σ'_p values which can be found in the technical litterature about Santos clay.

• Conclusions regarding the working tools

The fact is that there is no "off the shelf" practical tool available to back-analyze the monitoring data of embankment on soft soils with the working hypothesis which consists in considering that, in the field, primary consolidation and secondary consolidation occur simultaneously. This means that one still has to build his own tool before being able to start any such back-analysis.

As shown in item 10, the first tool which the authors built was the Bjerrum type abacus, plotting the strain, ε, *vs.* the vertical effective stress, σ'_v, in log scale, with the lines of equal values of strain rate, $\dot{\varepsilon}$, from the results of the special oedometer tests. But it was readily found that this tool was not usable for drainage distances different of the oedometer test one. Leroueil *et al.* (1985) had already warned about the *"Use and limitations"* of abacus built from oedometer tests results: "The rheological model proposed described by the two curves $\sigma'_p = f(\dot{\varepsilon}_v)$ and $\sigma'_v/\sigma'_p = g(\varepsilon_v)$ can be combined with a strain (or void ratio) permeability relation (ε_v - k or e - k), such as those described by Tavenas *et al.* (1983), to resolve problems of consolidation. It should be kept in mind, however, that the model has been established on small specimens and for strain rates usually encountered in the laboratory, and thus, for the moment, it must be used only under such conditions to interpret and understand clay behavior in the laboratory. It will probably be the basis for a reanalysis of the current practice for estimating settlements and settlement rates. However, before using this model for field applications where the strain rates are much lower and the clay layer much thicker, it is necessary to verify its validity under these conditions and in particular to determine how the σ'_p - $\dot{\varepsilon}_v$ curve extrapolates at low strain rates. A research programme on this problem is in progress at Laval University, Quebec."

As shown in item 11, the second tool which the authors built was the same type of abacus, but specifically built for the field conditions through extrapolating the laboratory abacus making use of Taylor and Merchant's theory. This second tool also failed to be usable.

The third tool which was tried did not really have to be built by the authors because it is already available, for the case of vertical drainage, although in the authors' knowledge it has never been used for this application before. The application of this tool needs that the final primary compression and the final secondary compression be known which, of course, asks for the reliable knowledge of the parameters provided by the high quality standard and special oedometer tests discussed above, that is C_c, C_r, σ'_p and the OCR value equivalent to the end of secondary consolidation.

Since the third tool is not applicable to the case of radial drainage and since, to the authors' knowledge, no analytical formulation of the evolution of secondary consolidation with time in the case of radial drainage can be found in the literature, then the authors built their fourth tool which is the "Pimary Barron + secondary pseudo Taylor and Merchant" as described in item 13.

In the light of all the above conclusions and considering the very good fit of the theoretical Taylor and Merchant curves with the measured compression curves under area 3 with vertical drainage and the very good fit of the theoretical "Primary Barron + secondary pseudo Taylor and Merchant" curves with the measured compression curves under areas 1 and 2 with radial drainage, it can be concluded that tool number 3 (Taylor and Merchant's theory for vertical drainage) and tool number 4 ("Primary Barron + secondary pseudo Taylor and Merchant" for radial drainage) did fulfill very satisfactorily their purpose to provide a trustworthy back-analysis of the measured compression curves of the SFL clay layers under the pilot embankment.

It is worth saying that in cases such as the one analyzed in this work, in which the stress increment is so that $\sigma'_{v0} < \sigma'_p < \sigma'_{vf}$, it is indispensable to take into consideration the variation of c_v and c_h values in the backanalysis in order to obtain a reasonable fitting between the theoretical and measured curves.

• Conclusions regarding the application of the results to the design of the improvement of the soft layer

It can be concluded, then, that the Taylor and Merchant theory can be used to predict the consolidation of the SFL clay layer with vertical drainage and the "Primary Barron + secondary pseudo Taylor and Merchant" procedure can be used to predict the consolidation of the SFL clay layer with radial drainage in any area of the Terminal, taking into account the proper local geometry and drainage conditions of the layer, as long as this prediction is done for various succeeding periods of time, using for each period the proper c_v (or c_h) value, estimated in function of the value of σ'_v applied during each period in the light of Fig. 38, although it might be expected that "the real value of the secondary compression might always be equal to or higher than the predicted one mainly in the middle of the process".

16. Final Comments

Based on the experience acquired during the five years which elapsed between the first soils report written in 2005 for the beginning of the basic design to the final interpretation of the pilot embankment data in 2010, the following comments come to the authors' minds:

• the soft marine Santos clay layer with SPT blow count from 0 to 4 named SFL (River lagoon sediments) is constituted of distinct layers, each with its specific compression and consolidation parameters, and has to be described and modeled as a number of layers as shown in Fig. 5,

• most routine oedometer tests which are performed on so called "undisturbed samples" fail to provide trustworthy values of compression and consolidation parameters and their only contributions to the knowledge of the subsoil conditions are the unit weight, the water content and the void ratio values,

• only high quality oedometer tests on good quality "undisturbed" samples provide trustworthy compressibility and consolidation parameters, and only oedometer tests with the highest achievable quality should be performed which implies that only proven first class soils investigation firms and laboratories should be contracted with their services closely supervised by the design engineer,

• special oedometer tests to determine the OCR value equivalent to the end of secondary consolidation should be performed for every design of embankments on soft clayey foundation,

• field c_v and c_h values are found to be smaller than or equal to (depending on the stress level) lab c_v values for the same effective stress level, and not the contrary,

• aging is the cause of overconsolidation which prevails on the dune action and sea level lowering for depths higher than 10 to 15 m in Barnabé Island area in the Santos harbour channel,

• all soft clay parameters obtained through Asaoka's method should be discarded and all data of embankment monitoring should be re-visited with the working hypothesis that primary consolidation and secondary consolidation occur simultaneously,

• practicing engineers are badly in need of reliable realistic working tools which they can use to back-analyze embankment monitoring and also to predict the behavior of the embankments which they design and build taking into account the simultaneous occurrence of primary and secondary consolidations,

• the literature versing on the field behavior of soft clay taking into account the simultaneous occurrence of primary and secondary compressions is very abundant and this is much more so than when Leroueil *et al.* (1985) wrote that "this abundant literature has modified neither the common practice based on the Terzaghi theory nor the way of thinking on clay behavior", however no practical tool has emerged from all this literature which can readily be used in common practice,

• in the lack of better practical available methods, the Taylor and Merchant's formulation and the "Primary Barron + secondary pseudo Taylor and Merchant" procedure used by the authors allow for reasonably reliable modeling of the soft clay field behavior, taking into account the simultaneous occurrence of primary and secondary consolidations, but since in Taylor and Merchant's own words, this formulation is "based largely on physical intuition" and "the main value of this theory is not in the expression of a secondary compression time law" it is to be hoped that, in the near future, some progress will be made in the understanding of the mechanism and in the expression of the evolution either of secondary consolidation or of total consolidation (without the need of a distinction between primary and secondary) with time,

• the lack of practical tools to take into account the simultaneous occurrence of primary and secondary consolidations has been, in the authors' understanding, the main hindrance to changes in common practice and this situation has much to do with the very little communication and lack of joint endeavour between practicing engineers and researchers.

Acknowledgments

The authors are grateful to EMBRAPORT in the person of Mr. Juvêncio Terra, for authorizing the use of the pilot embankment monitoring data to produce and publish this paper, and to Construtora Norberto Odebrecht in the person of Mr. Gilberto Gomes, who was always available to the authors to provide the instruments readings and all other relevant informations.

References

Aguiar, V.N. (2008) Características de Adensamento da Argila do Canal do Porto de Santos na Região da Ilha Barnabé. M.Sc. Thesis, COPPE/UFRJ, Rio de Janeiro, 223 pp.

Andrade, M.E.S. (2009) Contribuição ao Estudo das Argilas Moles da Cidade de Santos. M.Sc. Thesis, COPPE/UFRJ, Rio de Janeiro, 397 pp.

Asaoka, A. (1978) Observational Procedure of Settlement Prediction, Soils and Foundations, Japanese Society of Soil Mechanics Foundation Engineering, v.18:4, pp. 87-101.

Barron, R.A. (1948) Consolidation of fine-grained soils by drain wells. Transactions, ASCE, SM6, v. 113:2346, pp. 718-742.

Bjerrum, L. (1972) Embankments on Soft Ground, Proceedings of the Specialty Conference on Performance of Earth and Earth – Supported Structures, ASCE Soil Mechanics and Foundations Division, Purdue University, Lafayette, Indiana, USA, volume II, pp. 1-54.

Carvalho, S.R.L. (1997) Uma Teoria de Adensamento com Compressão Secundária. PhD Thesis, COPPE-UFRJ, Rio de Janeiro, 265 pp.

Christie, I.F. (1964) A Re-appraisal of Merchant's Contribution to The Theory of Consolidation, Géotechnique, v. 14:4, pp. 309-320.

Coutinho, R.Q. (2007) Characterization and Engineering Properties of Recife Soft Clays – Brazil, Characterization and Engineering Properties of Natural Soils, Proceedings of the Second International Workshop on Characterisation and Engineering Properties of Natural Soils, Singapore, 29 November-1 December 2006, K.K. Phoon, D.W. Hight, S. Leroueil, and T.S. Tan, Taylor & Francis Group, London, Chapter 12, pp. 2049-2100.

Feijó, R.L. (1991) Relação entre a Compressão Secundária, Razão de Sobreadensamento e Coeficiente de Empuxo no Repouso. M.Sc. Thesis, COPPE/UFRJ, Rio de Janeiro, 167 pp.

Feijó, R.L. & Martins, I.S.M. (1993) Relação entre a Compressão Secundária, OCR e K0. Proc. Simpósio Geotécnico Comemorativo dos 30 Anos da COPPE/UFRJ, COPPEGEO 93, COPPE/Federal University of Rio de Janeiro, Rio de Janeiro, pp. 27-40.

Garlanger, J.E. (1971) The Consolidation of Clays Exhibiting Creep Under Constant Effective Stress, Norwegian Geotechnical Institute, Internal Report, n. 50302, Oslo, pp.71-78.

Gibson, R.E. & Lo, K.Y. (1961) A Theory of Consolidation for Soils Exhibiting Secondary Compression, Publication Nº. 41, Norwegian Geotechnical Institute, Oslo, pp. 1-16.

Gonçalves, H.H.S. (1992) Análise Crítica Através de Modelos Visco-Elásticos dos Resultados de Ensaios de Laboratório para Previsão de Recalques dos Solos da Baixada Santista. PhD Thesis, USP, São Paulo, 184 pp.

Holl, D.L. (1940) Stress Transmission in Earth, Proc. High Res. Board, v. 20, pp. 709-721.

Ladd, C.C. & De Groot, D.J. (2003) Recommended Practice for Soft Ground Characterization, Arthur Casagrande Lecture, Proceedings of the 12th Panamerican Conference on Soil Mechanics and Geotechnical Engineering, Massachusetts Institute of Tecnology, Cambridge, June 22-25, pp. 1-55.

Ladd, C.C. (2008) Commentary: Soft Ground Geotechnics. Geo-Strata – Geo Institute of ASCE, v. 9:2, March/April 2008, pp. 10-11.

Larsson, R.; Bengtsson, P.E. & Eriksson, L. (1997) Prediction of Settlements of Embankments on Soft, Fine-Grained Soils – Calculation of Settlements and Their Course with Time, Information 13E, Swedish Geotechnical Institute, Linköping, 52 pp.

Leroueil, S.; Kabbaj, M.; Tavenas, F. & Bouchard, R. (1985) Stress-Strain Rate Relation for the Compressibility of Sensitive Natural Clays, Geotechnique, v. 35:2, pp. 159-180.

Martins, I.S.M. (2005) Algumas Considerações Sobre Adensamento Secundário. Conference given at Clube de Engenharia, Rio de Janeiro, 47 pp.

Martins, I.S.M.; Santa Maria, P.E.L. & Santa Maria, F.C.M. (2009) Laboratory Behaviour of Rio de Janeiro Soft Clays, Part 1: Index and Compression Properties, Soils and Rocks, v. 32:2, pp. 100-103.

Massad, F. (1989) Settlements of Earthworks Construction on Brazilian Marine Soft Clays in the Light of their Geological History, Proc. XII International Conference on Soils Mechanics and Foundation Engineering, Rio de Janeiro, v. 3. pp. 1749-52.

Massad, F. (2009) Solos Marinhos da Baixada Santista, Características e Propriedades Geotécnicas. Oficina de Textos, São Paulo, 247 pp.

Orleach, P. (1983) Techniques to Evaluate the Field Performance of Vertical Drains, Master Thesis, Massachusetts Institute of Technology, 159 pp.

Poulos, H.G. & Davis, E.H. (1974) Elastic Solutions for Soil and Rock Mechanics, John Wiley and Sons, New York, 411 pp.

Saye, S.R. (2001) Assessment of Soil Disturbance by The Installation of Displacement Sand Drains and Prefabricated Vertical Drains, GSP n. 119, pp. 325-362.

Schofield, A. & Wroth, P. (1968) Critical State Soil Mechanics, McGraw-Hill, London, 310 pp.

Tavenas, F.; Jean, P.; Leblond, P. & Leroueil, S. (1983) The Permeability of Natural Soft Clays: Part II, Permeability Characteristics. Can. Geotech. J. v. 20:4, pp. 645-660.

Taylor, D.W. & Merchant, W. (1940) A Theory of Clay Consolidation Accounting for Secondary Compression, Journal of Mathematics and Physics, v. 19:3, pp. 167-185.

Taylor, D.W. (1948) Fundamentals of Soils Mechanics, Wiley International Edition. J. Wiley & Sons, Cambridge, Massachusetts, pp. 700.

Teh, C.I. & Houlsby, G.T. (1991) An Analytical Study of The Cone Penetration Test in Clay, Géotechnique, v. 41:1, pp. 17-34.

Terzaghi, K. & Frohlich, O.K. (1936) Theorie der setzung von tonschichten. Franz Deuticke, Vienna (translated into French: Théorie des Tassements des Couches Argileuses. Dunod, Paris, 1939), 166 pp.

Varaksin, S. (2010) Vacuum Consolidation, Vertical Drains for the Environment Friendly Consolidation of Very Soft Polluted Mud at the Airbus A-380 Factory Site, Symposium on New Techniques for Design and Construction in Soft Clays, Guaruja, Oficina de Textos, São Paulo, pp. 87-102.

Vieira, L.O.M. (1988) Contribuição ao Estudo de Adensamento Secundário. M.Sc. Thesis, COPPE/UFRJ, Rio de Janeiro, 137 pp.

List of Symbols

w: Natural water content

z: Depth

γ: Unit weight

H: Layer thickness

H_d: Drainage distance

LL: Liquid limit

PI: Plasticity index

a_v: Coefficient of compressibility (primary + secondary) (Taylor & Merchant)

a'_v: Coefficient of primary compressibility (Taylor & Merchant)

b: Berm thickness

C_c: Compression index

C_e: Expansion index

C_r: Recompression index

$C\alpha$, $C_{\alpha\varepsilon}$: Coefficient of secondary consolidation (according to the theory which considers secondary consolidation to occur at the end of primary consolidation)

c_v: Vertical coefficient of consolidation

c_{v1}: Vertical coefficient of consolidation in the recompression domain

c_{v2}: Vertical coefficient of consolidation in the normally consolidation domain

c'_v: Vertical coefficient of consolidation obtained through Asaoka's method

c_h: Horizontal coefficient of consolidation

c_{h1}: Horizontal coefficient of consolidation in the recompression domain

D, Hd: Vertical drainage distance

D_{eq}: Equivalent vertical drainage distance

e_0: Initial void ratio (after sampling)

e: Void ratio

e_i: Initial void ratio corresponding to initial (*in situ*) vertical effective stress

e_p: Final void ratio at end of primary consolidation (without secondary)

e_s: Final void ratio at end of primary and secondary consolidation

El.: Elevation

F: Secondary compression factor

k: Horizontal permeability coefficient of undisturbed soil

k_s: Horizontal permeability coefficient of smear zone

r: Ratio of the primary settlement over the total settlement

r_s: Radius of the smear zone

r_w: Radius of the drain

R: Mean radial drainage distance

S_u: Undrained in-situ shear strength

S_u(VT): Undrained shear strength obtained from the vane test

T: Time factor

t: Time

U (or U_p or $U_{primary}$): Primary consolidation ratio

U_p*: Primary consolidation ratio at t = 220 days

U_p*': Primary consolidation ratio at t = 220 days obtained through Asaoka's method

U_t (or $\overline{B}$): Mean primary consolidation ratio at time t

U_{p+s}: Aggregate consolidation ratio (apud Taylor and Merchant)

u_{hid}: Hydrostatic water pressure

$\overline{U}_p$: Average primary consolidation ratio

μ: Coefficient of secondary compression (apud Taylor & Merchant)

W.L.: Water level

ε (or ε' or ε_v): Vertical strain

$\dot{\varepsilon}$ (or $\dot{\varepsilon}_v$): Vertical strain rate

$\dot{\varepsilon}_{0p}$: Expected vertical strain rate in the early phase of terminal operation

ε_{0p}: Expected future vertical strain during terminal operation

$\dot{\varepsilon}_t$: Measured vertical strain rate in individual soft clay layer at time t

ε_t (or ε'_t): Measured vertical strain in individual soft clay layer at time t

ε_f: Final vertical strain corresponding to primary + secondary consolidation

ε_p: Final vertical strain corresponding to primary consolidation

ε_{pt}: Vertical strain due to primary consolidation at time t

ε_s: Final vertical strain corresponding to secondary consolidation

ε_{st}: Vertical strain due to secondary consolidation at time t

σ_v: Total stress

$\sigma_v - u_{hid}$: Pseudo final effective stress

σ'_p: Preconsolidation stress

σ'_v (or P): Vertical effective stress

σ'_{vi}: Initial vertical effective stress

σ'_{vf}: Final effective vertical stress

σ'_{vt}: Mean effective stress in the layer at time t

$\Delta\sigma_v$ (or Δσ): Vertical stress increase

$\Delta\sigma'_v$: Effective vertical stress increase

$\Delta\sigma'_{v1}$: Vertical effective stress change at removing of surcharge

$\Delta\sigma'_{v2}$: Vertical effective stress increase during operation

ΔH: Layer compression

ΔH_n, ΔH_{n-1}: Layer compression of orders n and n-1 in Asaoka's construction

ΔH*: Layer compression at t = 220 days

ΔH_p: Layer primary compression

$\Delta H'_p$: Layer primary compression obtained through Asaoka's method

ΔH_{pj}: Primary compression at end of period j

ΔH_s: Layer secondary compression

ΔH_{sj}: Secondary compression at end of period j

ΔH_t: Layer total compression

ΔH_{tj}: Total (primary + secondary) compression at end of period j

ΔH_m: Measured layer compression in October 2009

$(\Delta H_p)'$: Pseudo final primary compression

$(\Delta H_s)'$: Pseudo final secondary compression

$(\Delta H_t)'$: Pseudo final total compression

Δe: Variation of void ratio

Δe_p: Variation of void ratio corresponding to primary compression

Δe_s: Variation of void ratio corresponding to secondary compression

$\Delta\varepsilon_v$: Vertical strain increase

Δt: Time increment

∂e: Infinitesimal void ratio increment

∂t: Infinitesimal time increment

α: Slope of stress *vs.* void ratio (primary + secondary compression) curve (Taylor & Merchant)

α': Slope of stress *vs.* void ratio (primary compression curve Taylor & Merchant)